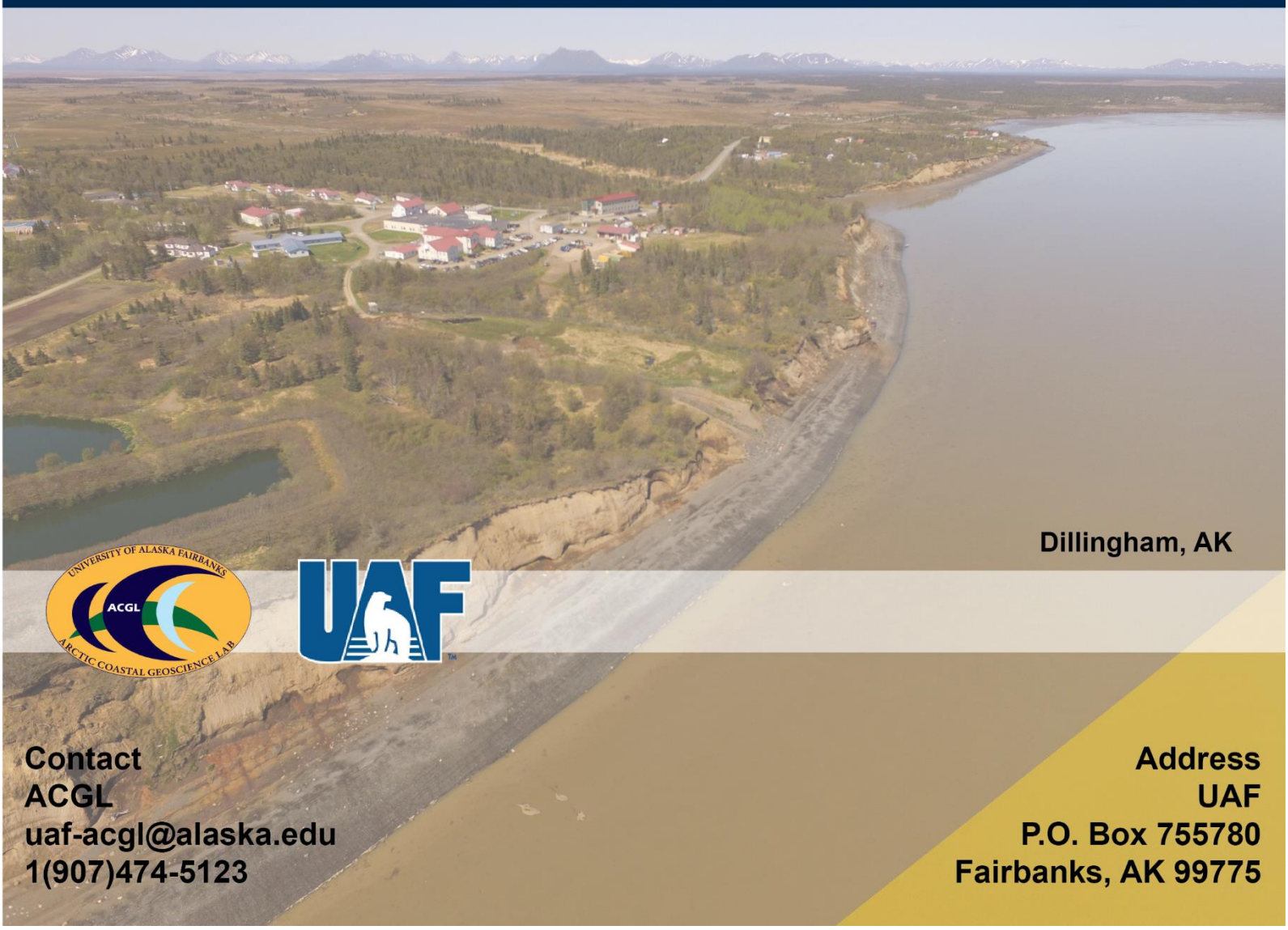
Dillingham Coastal Hazard Analysis

Arctic Coastal Geoscience Laboratory (Ver. March 2022)

Reyce Bogardus, Richard Buzard, Gabe Dunam, Roberta Glenn, Michael Letzering, Sue Flensberg, CaSandera Johnson, Renee Roque, Harper Baldwin, Jessie Christian, Courtenay Carty, Desi Bond, Matthew Balazs, Chris Maio



Dillingham, AK

Contact
ACGL
uaf-acgl@alaska.edu
1(907)474-5123

Address
UAF
P.O. Box 755780
Fairbanks, AK 99775

STATEMENT OF INTENT

This report is meant to contribute accurate information and high-resolution map and data products to inform erosion and flooding mitigation efforts. It is our goal that this report will aid in local decision making, provide maps and graphics for research funding opportunities, and be an information source for FEMA Hazard Mitigation Plans. We have compiled an assortment of existing data sources (DGGS, UAF-SNAP, etc.) that provide information on current and projected environmental changes. Additionally, numerous datasets have been collected, processed, and analyzed by the ACGL. This work was primarily carried out by undergraduate and graduate students within the ACGL, providing training opportunities for the next generation of geoscientists. Local environmental coordinators have also played a major role in the baseline surveys, operation of erosion monitoring sites, as well as this document. All data and products will be provided by the ACGL upon request. This report is meant to supplement more detailed geotechnical surveys, such as those carried out by contracted engineering firms.

ACKNOWLEDGMENTS

This research has been supported and/or funded through multiple contributors. These include local Tribal Environmental Programs through the Environmental Protection Administration (EPA) Indian General Assistance Program (IGAP), Alaska Sea Grant (ASG), the National Science Foundation (NSF) POLARIS project, the Bristol Bay Native Association (BBNA), the Bureau of Indian Affairs (BIA), the University of Alaska Fairbanks (UAF) Geophysical Institute, and the Alaska Division of Geological and Geophysical Surveys Coastal Hazards Program (DGGS). We also thank the long-term contributions made by Susan Flensburg, Gabriel Dunham, and Nicole Kinsman.

We would like to thank the Curyung Tribe Environmental Department as well as other community members for their continued efforts to collect monitoring data, their local observations, and assistance during field work. We greatly appreciate your knowledge and support and look forward to our continued collaboration.

DRAFT

DISCLAIMER

The hazard assessments in this report are based on a compilation of data we collected, as well as the data made available to the Arctic Coastal Geoscience Lab (ACGL) through external agencies and bodies. The maps and products within have been created from analysis of this information using modern techniques and based on the best information currently available. However, they do not necessarily show the greatest extent of coastal flooding or erosion suffered in the past, or likely to be suffered in the future. There are also other uncertainties associated with each analysis and mapping product. As such, the ACGL does not warrant or represent that the maps are free from errors or omissions, nor do we accept any liability in relation to the quality or accuracy of the flood and erosion maps. In particular, the ACGL does not warrant that land not shown as being subject to inundation or erosion, is free from flood waters or erosional processes.

The extent of coastal flooding maps is based on the coastal topography at the time of survey. Changes in coastal landform that have occurred since the date of survey, as well as potential future landform change are not reflected in the coastal flood mapping. The maps reflect flooding and erosion associated with coastal processes, and as such do not represent flooding and erosion caused by storm rainfall, including surface run off, storm water network overflow, and river flooding.

We have not assessed or mapped coastal hazards outside of the surveyed areas shown in this report. For areas where only one type of coastal hazard (flooding / erosion) has been mapped, it should be assumed that any unmapped coastal hazard has not been assessed. Where only coastal flood risk has been mapped it should not be assumed that no coastal erosion hazard exists, and vice versa.

The tsunami inundation map has been completed using the best information available and is believed to be accurate; however, its preparation required many assumptions. Actual conditions during a tsunami may vary from those assumed, so the accuracy cannot be guaranteed. Areas inundated will depend on specifics of the earthquake, any earthquake-triggered landslides, on-land construction, tide level, local ground subsidence, and may differ from the areas shown on the map. Information on this map is intended to permit state and local agencies to plan emergency evacuation and tsunami response actions. The map is not appropriate for site-specific use or for land-use regulation. Interpretation of the tsunami inundation map(s) by qualified experts is strongly recommended.

Finally, this work is preliminary and is subject to revision. It is being provided due to the need for timely "best science" information. Accordingly, these maps should not be relied upon as the sole basis for the making of any decision in relation to potential coastal hazard risk. The assessment is provided on the condition that neither the ACGL nor the University of Alaska Fairbanks may be held liable for any damages resulting from the authorized or unauthorized use of the assessment.

DRAFT

TABLE OF CONTENTS

Table of Contents **3**
List of Figures **4**
List of Tables **5**
Acronyms and Abbreviations **6**
Glossary **7**
1. Local Narrative **8**
2. Geographic Overview **8**
2.1 Bristol Bay Region 8
2.2 Dillingham 9
2.3 Community Information 11
2.3.1 Infrastructure Description 11
2.3.2 Transportation 15
2.3.3 Economy 15
2.4 Geologic Setting 15
2.5 Climate and Meteorology 19
2.5.1 Temperature Regime 19
2.5.2 Wind Regime 22
2.5.3 Storm Regime 24
2.6 Oceanographic Setting 25
2.6.1 Tides and Currents 25
2.6.2 Wave Climate 28
2.7 Sea ice 29
3. Natural Hazards and Mitigation Efforts **32**
3.1 Description of Hazards 32
3.1.1 Erosion 32
3.1.2 Flooding 35
3.1.3 Earthquakes 39
3.1.4 Landslides 41
3.1.5. Tsunami 41
3.1.6 Sea Level Change 42
3.2 Past/Ongoing Mitigation Efforts 43
4. Data Products and Assessment Tools **44**
4.1 Previous Assessments 44
4.2 Reference Datasets 46
4.2.1 Ground Control Points and Checkpoints 46
4.2.2 Benchmarks 47
4.2.3 Digital Surface Models and Orthomosaics 48
4.2.4 Tidal Datums 49
4.2.5 Bathymetry 50
4.3 Repeat Datasets 50
4.3.1 Shoreline Indicator Position 51
4.3.2 Stake Measurements 51
4.3.3 Cross Shore Elevation Profiles 54
4.3.4 Timelapse Photography 56
4.4 Hazard and Exposure Assessments 58

DRAFT

4.4.1 Flood Hazard Map 58
4.4.2 Infrastructure Exposure Maps 58
4.4.3 Shoreline Change Analysis 60
5. Identified Coastal Hazard Areas 62
6. Summary of Community Threats and Resiliency 66
6.1. Summary of Threats 66
7. Data Gaps and Future Work 66
7.1. Priority Data Gaps 66
7.2. ACGL Future Work 66
8. Citations 67

LIST OF FIGURES

Figure 1. Regional context of the Dillingham, AK study site. 10
Figure 2. Aerial view of the Dillingham Harbor taken in 2009. 11
Figure 3. Bristol Alliance Fuel facilities as seen behind the eroding bank. 12
Figure 4. Aerial image of the Kanakank Hospital and sewage lagoons. 13
Figure 5. Map showing the building and utility infrastructure of Dillingham. 14
Figure 6. Physiographic provinces of southwestern Alaska after Wahrhaftig (1965).. .. 17
Figure 7. Generalized surficial geology of the Dillingham area 18
Figure 8. Annual temperature increase in Alaska between 1970 and 2019. 20
Figure 9. Autumn temperature increase in Alaska between 1969 and 2018. 20
Figure 10. Mean summer temperatures in Dillingham between 1973 and 2019 21
Figure 11. Mean fall temperatures in Dillingham between 1973 and 2019 22
Figure 12. Averaged monthly wind roses for Dillingham (1973-2019). 23
Figure 13. Storm track density climatology in the North Pacific from 1948/49 to 2008. 24
Figure 14. Graphic representation of relative strength of component marine energy ... 26
Figure 15. Example time series (12/15/21 – 12/20/21) of water level 27
Figure 16. Tidal datum computed for Dillingham using NOAAs online data viewer. 28
Figure 17. Sea ice concentrations for the month of March between 1850 and 2018 29
Figure 18. Average monthly sea ice extent in Bristol Bay from 1981-2010. 30
Figure 19. Bench ice along the city dock. Image taken Feb, 2020. 31
Figure 20. Components of a sediment budget for a sandy coast. 33
Figure 21. City Dock Side erosion at the park. Source: USACE, 2009. 34
Figure 22. Erosion at the city sewage lagoon.. 34
Figure 23. Diagram showing the various components of Total Water Level (TWL). 36
Figure 24. City of Dillingham's Identified Flood Areas by AECOM. 37
Figure 25. Dillingham Harbor during a storm in August 2005. 38
Figure 26. Earthquake probability in Alaska 40
Figure 27. Tsunami hazard map of Dillingham 41
Figure 28. Predicted uplift rates with glacial isostatic adjustment subtracted 42
Figure 29. City lagoon model collected May 2021. 48
Figure 30. Hospital lagoon model collected October 2021. 48
Figure 31. Map of erosion monitoring sites and stake measurement transects 52

DRAFT

Figure 32. Plotted stake ranging measurements from site 1, sewage lagoon. 53
Figure 33. Plotted stake ranging measurements from site 2, peat meadow. 53
Figure 34. Site map showing the location of cross shore elevation profiles..... 54
Figure 35. Example cross shore profile from the City Sewage Lagoon 55
Figure 36. Example cross shore profile from the City Sewage Lagoon 55
Figure 37. Example time-lapse picture of erosion monitoring site 1 57
Figure 38. Example time-lapse picture of erosion monitoring site 2 57
Figure 39. Shoreline change map of the Dillingham area.. 59
Figure 40. Shoreline change and erosion projection map of the Dillingham area.. 61
Figure 41. Shoreline change map of the city sewage lagoon. 63
Figure 42. Shoreline change map of the Dillingham area. 64
Figure 43. Shoreline change map of the Dillingham area.. 65

LIST OF TABLES

Table 1. Provides Dillingham's total building stock values 14
Table 2. Table of documented flooding events in Dillingham.. 39
Table 3. Summary of ACGL community visits and field work. 45
Table 4. Summary of GPS survey points per product type and date. 46
Table 5. NGS benchmarks within 10km of Dillingham 47
Table 6. Overview of compiled bathymetry surveys of Dillingham. 50
Table 7. Summary of aerial and satellite imagery used for shoreline delineation. 60
Table 8. Summary of data gaps at Dillingham. 66

DRAFT

ACRONYMS AND ABBREVIATIONS

ACCAP	Alaska Center for Climate Assessment and Policy
ACGL	Arctic Coastal Geoscience Laboratory
ADLWD	Alaska Department of Labor and Workforce Development
AHAP	Alaska High Altitude Photography
AIJ	Alaska Institute for Justice
AOOS	Alaska Ocean Observing System
ASOS	Automated Surface Observing System
DCRA	Division of Community and Regional Affairs
DGGS	Division of Geological and Geophysical Surveys
DSAS	Digital Shoreline Analysis System
DSM	Digital Surface Model
ESRI	Environmental Systems Research Institute
GIS	Geographic Information System
GLONASS	Global Orbiting Navigation Satellite System
GNSS	Global Navigational Satellite System
MHHW	Mean Higher High Water
MHW	Mean High Water
MSL	Mean Sea Level
NASA	National Aeronautics and Space Administration
NAVD88	North American Vertical Datum of 1988
NIR	Near infrared
NOAA	National Oceanic and Atmospheric Administration
NSM	Net Shoreline Movement
RGB	Red, Green, Blue
RSLR	Relative Sea Level Rise
RTK	Real-time Kinematic
SECD	Strategic Economic and Community Development
SfM	Structure from Motion
SVTM	Single Value Threshold Map
UAV	Unmanned Aerial Vehicle
USACE	United States Army Corps of Engineers
USGS	United States Geological Survey
UTM	Universal Transverse Mercator
WCI	Weighted Confidence Interval
WEAR	Waste Erosion Assessment and Review
WIS	Wave Information Study
WLR	Weighted Linear Regression
WMO	World Meteorological Organization
WR2	Weighted R Squared

DRAFT

GLOSSARY

Definitions were pulled from the United Nations Office for Disaster Risk Reduction.

Capacity the combination of all the strengths, attributes and resources available within an organization, community or society to manage and reduce disaster risks and strengthen resilience.

Disaster risk (referred to as risk): the potential loss of life, injury, or destroyed or damaged assets which could occur to a system, society or a community in a specific period of time, determined probabilistically as a function of hazard, exposure, vulnerability and capacity.

Disaster risk assessment (referred to as risk assessment): A qualitative or quantitative approach to determine the nature and extent of disaster risk by analyzing potential hazards and evaluating existing conditions of exposure and vulnerability that together could harm people, property, services, livelihoods and the environment on which they depend.

Exposure the situation of people, infrastructure, housing, production capacities and other tangible human assets located in hazard-prone areas.

Hazard a process, phenomenon or human activity that may cause loss of life, injury or other health impacts, property damage, social and economic disruption or environmental degradation.

Mitigation the lessening or minimizing of the adverse impacts of a hazardous event.

Resilience the ability of a system, community or society exposed to hazards to resist, absorb, accommodate, adapt to, transform and recover from the effects of a hazard in a timely and efficient manner, including through the preservation and restoration of its essential basic structures and functions through risk management.

Vulnerability the conditions determined by physical, social, economic and environmental factors or processes which increase the susceptibility of an individual, a community, assets or systems to the impacts of hazards.

DRAFT

1. LOCAL NARRATIVE

2. GEOGRAPHIC OVERVIEW

2.1 BRISTOL BAY REGION

Bristol Bay is the eastern edge of the Bering Sea in southwest Alaska. The region contains approximately 7,500 residents and encompasses the Dillingham census area, Bristol Bay and Lake and Peninsula Boroughs, as well as a portion of the Aleutians East Borough (NWF, 2021). The greater watershed is home to twenty-five federally recognized tribal governments, fourteen of which are located within the Nushagak River and Kvichak River watersheds, the two largest of Bristol Bay's six major river basins (EPA, 2021).

Bristol Bay supports the largest sockeye salmon fishery in the world, with approximately 46% of the average global abundance of wild sockeye salmon (EPA, 2021). As a result, the region's economy is almost exclusively driven by a commercial and sport fishing industry that employs roughly 15,000 people and is currently valued at $2.2 billion. Annual commercial harvest for the most recent 20 years (2000–2019) averaged 27.0 million sockeye, 40,200 Chinook, 1.1 million chum, 510,000 pink (even-years only), and 96,400 coho salmon (Tiernan et al., 2021).

Such large-scale harvest equates to a vast network of fishing infrastructure across the region along coasts, rivers, and lakes (Buzard et al., 2019). This includes privately owned set net sites, public access roads and dock facilities, as well as commercially owned fish processing plants and dock facilities. This regional dependence on fishing means that coastal change is especially relevant to the residents' livelihood, wellbeing, and culture. Many communities within Bristol Bay have observed detrimental coastal change, such as loss of infrastructure, land access corridors, subsistence sites, and cemeteries (USACE, 2009; Smith and Sattineni, 2016; Melvin et al., 2017).

DRAFT

2.2 DILLINGHAM

As stated in Dillingham's 2016 Hazard Mitigation Plan, Dillingham is located at the head of Nushagak Bay at the confluence of the Wood and Nushagak Rivers (**Figure 1**). Dillingham is surrounded by 1.6 million acres of Wood-Tikchik State Park, the largest state park in the United States.

Consistent with its geological history, the topography of Dillingham is a mix of wet lowlands, gentle hills, and moraine deposits. There are a few areas with slopes too steep for development. Steep coastal bluffs occur at several locations along the Nushagak River below the core town site, most notably at the end of Squaw Creek Road, extending through Kanakanak Beach and adjacent to the Bristol Bay Area Health Corporation facility. Other steep bluffs occur beyond the end of Wood River Road, along the western bank of the Wood River. These steep-sided waterfront slopes are erosion-prone, offer poor access and limit the feasible sites for development of marine transportation facilities. Apart from these areas, slopes present severe limitations for development on some of the steeper back-slopes of hills and some of the steep slopes that run along drainages. Forested areas of moderate slope generally reflect favorable surface drainage (Dillingham HMP, 2016).

The City of Dillingham was once covered by glaciers, and the topography of the area is characteristic of areas where deposition by continental glaciers occurred. The landscape consists of rolling hills with many irregularly shaped moraine knolls and ridges separated by flat, wetlands and muskeg. The upland moraine hills are covered with a thick layer of silty, wind-laid material called loess - a mixture of silt blown from unvegetated floodplains and hills adjacent to the melting glaciers, and volcanic ash from the Aleutian Range to the east and south. Beneath this mantle of loess, the substratum is mostly coarse grained sand and gravel.

DRAFT

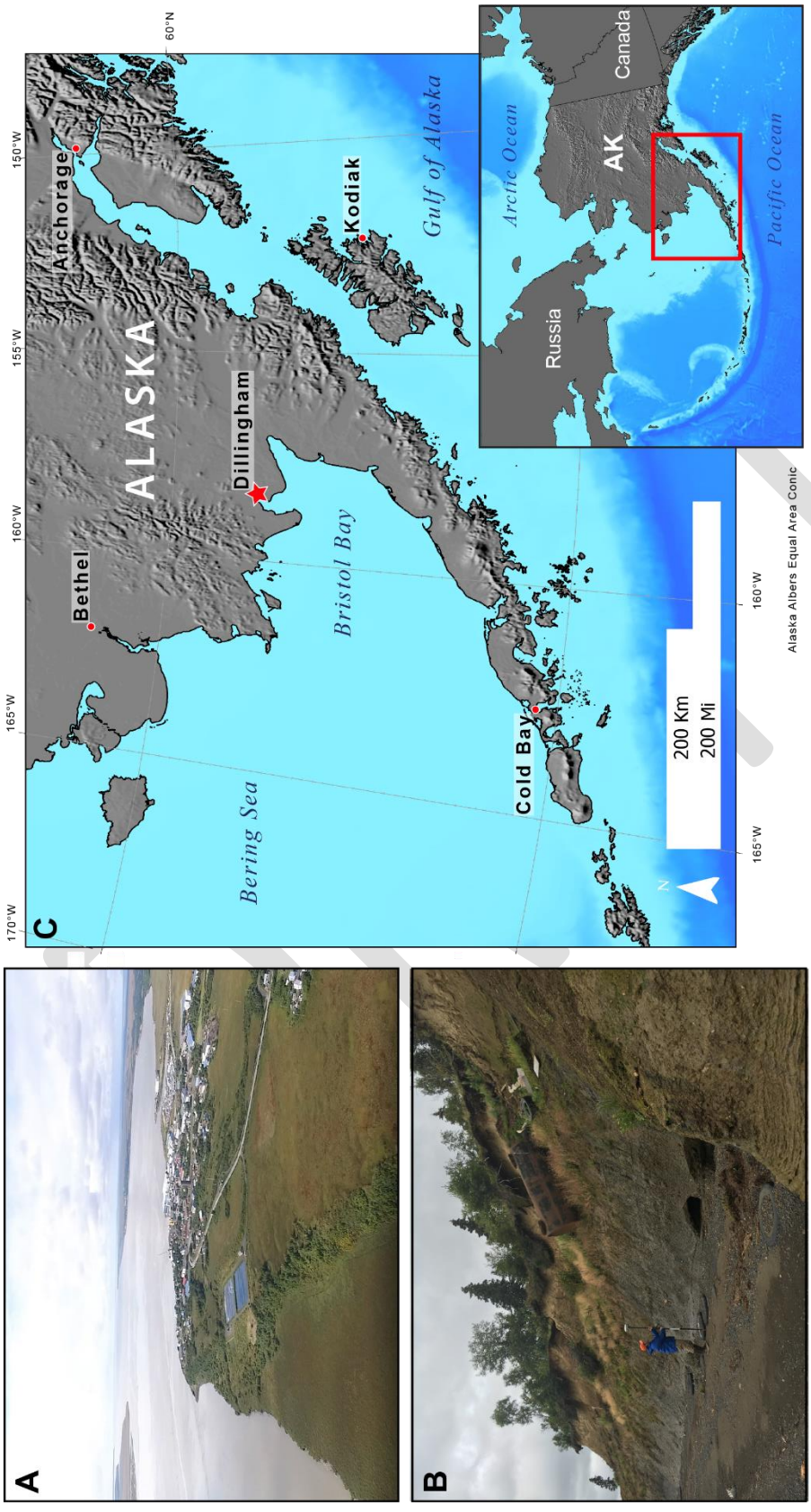


Figure 1. Regional context of the Dillingham, AK study site. (A) Aerial image showing the city sewage lagoon (foreground) and main commercial section of Dillingham (background), (B) Image showing a typical bluff shore along many portions of coastline at Dillingham, and (C) Regional map showing Dillingham's location within Bristol Bay.

2.3 COMMUNITY INFORMATION

The Dillingham area was first settled by Yup'ik Eskimo peoples who trace their ancestry back to the migration of Asiatic peoples across the Bering Land Bridge during the last Ice Age, 15,000 to 20,000 B.C. The first contact with Europeans occurred sometime between 1791 and 1824 as explorers, fur traders, and Russian Orthodox missionaries arrived in the area. Commercial fisheries developed after 1883 which had a tremendous influence on the population of the area, attracting Asian, Scandinavian, and Italian fishermen and cannery workers (Dillingham HMP, 2016).

The community is now a highly mixed population of non-Natives, Yup'ik, Aleut, and Athabascan peoples. Approximately 66 percent of the population possesses a Native heritage. Population growth has fluctuated over the years, with the highest growth beginning in the 1960s with a steady climb to today's population of approximately 2,431. This population grows to nearly double during the summer commercial fishing and tourism months.

2.3.1 Infrastructure Description

Docks/Harbors

With the only protected boat harbor in Bristol Bay, Dillingham serves as the center of the fishery (USACE, 2009) (**Figure 2**). The Dillingham All-Tide Dock is the primary entry and landing point for goods arriving from Seattle, Anchorage, and points in between for the communities of the Nushagak River and Togiak. The dock was constructed in 2004 and has seen a steady increase in barge traffic and materials delivered and fish products shipped out (Dillingham HMP, 2016).



Figure 2. Aerial view of the Dillingham Harbor taken in 2009. Image credit: USACE, 2009

Fuel tank farm

Bristol Alliance Fuels AF owns the land to the west of the harbor and the fuel facilities, which supply about half of the city's avgas, unleaded gasoline, jet fuel, diesel fuel, and home heating oil (**Figure 3**). BAF is the largest fuel facility in the Bristol Bay area. BAF is the major fuel supplier to the southwestern region of Alaska. BAF stores fuel for Crowley Marine barges so that Crowley can avoid sending large barges upriver and bottoming out in shallow spots. BAF supplies fuel to residents in the region for operating their boats and all terrain vehicles and, when the need arises, they also supply surrounding communities such as Aleknagik, Manokotak, Clarks Point, and Koliganek (Dillingham HMP, 2016).



Figure 3. Bristol Alliance Fuel facilities as seen behind the eroding bank (USACE, 2009).

Hospital

The Kanakanak Hospital is located 5.7 miles south of Dillingham and approximately 2.7 miles from the Dillingham Airport, at the end of Kanakanak Road (**Figure 4**). The Kanakanak Community Health Clinic is a 16-bed facility providing 24-hour medical, pediatric and obstetrical care. The hospital is fully accredited by The Joint Commission. Offices for several BBAHC's ancillary departments - Community Health Aide Program, Emergency Medical Services. Also located on hospital grounds are a pre-natal boarding home, the Substance Use Disorder facility, Behavioral Health Center and a new twelve station Dental building which was built in 2016. A limited number of apartments for qualifying permanent and temporary employees are also located on the compound. Housing is available and assigned using a priority list for employees who are on-call and need to be at the hospital for emergencies. Located off-compound but close by are WIC and the Infant Learning Program. Also Kanakanak House, headquarters to BBAHC's Environmental Health and Injury Prevention programs (Dillingham HMP, 2016).



Figure 4. Aerial image of the Kanakank Hospital and sewage lagoons. Image taken in May, 2021.

Sewage Lagoon

The Dillingham Sewage Lagoon is a 2 cell, unlined, aerated lagoon. The system was designed by CH2MHill, approved for construction by the Department of Environmental Conservation in 1986, and constructed in 1989. The Dillingham lagoon is authorized to discharge 273,000 gallons per day to the Nushagak River, by the Alaska General Permit AKG 573000, Authorization AKG573004 (Dillingham HMP, 2016).

Roads

The Dillingham roadway network consists of a total of 50 miles of roadway, including 15 miles of paved road within Dillingham itself, and 23 miles of paved road to Aleknagik (**Figure 5**). There are also several miles of paved road from Dillingham to the airport and to Kanakanak. The four main roadways in Dillingham include Kanakanak Road, Wood River Road, Aleknagik Lake Road, and Waskey Road (Dillingham HMP, 2016).

Other

The city contains well over 1,000 structures (**Figure 5**) with values in the hundreds of millions (**Table 1**).

Table 1. Provides Dillingham's total building stock values; summarized by occupancy class. Source: Dillingham 2016 Hazard Mitigation Plan

Structure Type	Quantity	Estimated Value ($)
Residential	1,047	391,839,750
Government	31	36,412,077
Commercial	14	83,177,859
Industrial	10	17,778,328
Religious/Non-profit	14	558,200
Education	6	24,200,203
Utilities	19	12,777,530
Total	**1,141**	**$455,120,485**

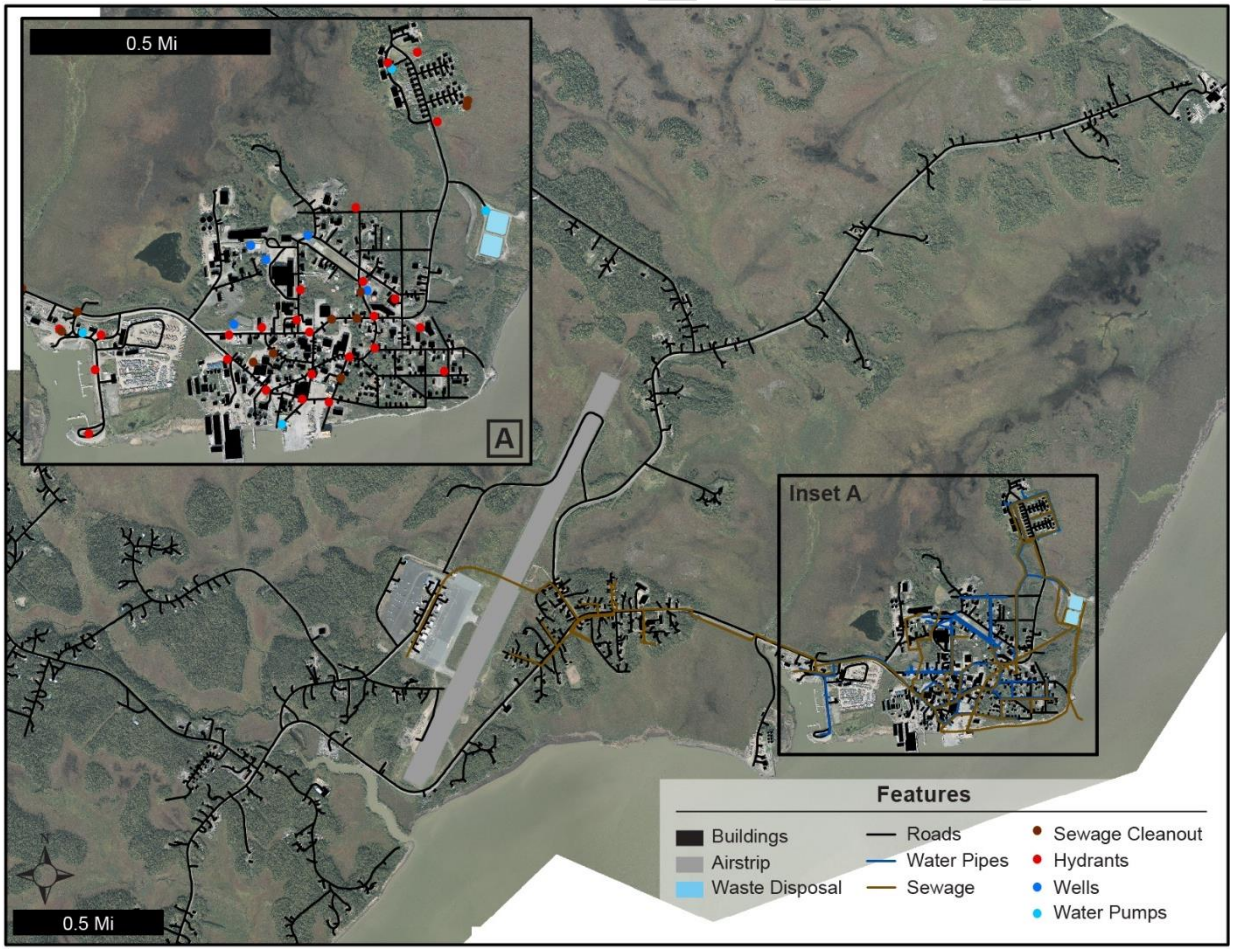


Figure 5. Map showing the building and utility infrastructure of Dillingham.

2.3.2 Transportation

Dillingham can only be reached by air and sea. The State-owned airport provides a 6,404 feet ft long by 150 ft wide paved runway and flight service station. Regular jet service is available from Anchorage, although the town's only passenger jet service, Alaska Airlines, cut back their Dillingham operations from year-round to summer only as of fall 2007. A seaplane base is available 3 miles west at Shannon's Pond and a heliport is available at Kanakanak Hospital. In 2007, four freight airlines served Dillingham; thirteen charter services served smaller communities from Dillingham; and two passenger airlines connected southwest Alaska residents from Bristol Bay and points south and west to King Salmon and Anchorage (Dillingham HMP, 2016).

The city operates a Small Boat Harbor during the summer, an all-tide dock boat harbor and boat launch facilities. Two private companies provide boat haul-out and storage services. Two barge lines make scheduled trips from Seattle. There is a 23-mile State of Alaska-maintained paved road to Aleknagik; constructed in 1960 and paved to the city limits in 1998. The road also had a paved pedestrian and bike path alongside the Aleknagik Lake Road up to mile 2. The pavement was extended to Aleknagik Lake and the bike path finished from the Dillingham Townsite to the Lake Road in 2004 (Dillingham HMP, 2016).

2.3.3 Economy

The economy of Dillingham employs 1.13k people. The largest industries in Dillingham, AK are Health Care & Social Assistance (316 people), Public Administration (160 people), and Educational Services (118 people), and the highest paying industries are Management of Companies & Enterprises ($83,750), Professional, Scientific, & Management, & Administrative & Waste Management Services ($77,083), and Administrative & Support & Waste Management Services ($75,833).

As of 2016, fifteen different fish processors operate in the Nushagak District, southeast of Dillingham. Of those, two major processors Peter Pan Seafoods & Icicle Seafoods operates processing plants onshore in Dillingham. Six other major processors, Ocean Beauty, Trident, and Leader Creek, Copper River, Ekuk Fisheries, Alaska's Best, Silver Bay and Red Salmon, coordinate their operations on floating processors in Dillingham's fishing district. Additionally, five catcher-processors had direct marketing out of the Nushagak District (Dillingham HMP, 2016).

Dillingham also offers non-fishery related employment and income opportunities. The University of Alaska Fairbanks' Bristol Bay Campus is based in Dillingham. This, together with the city's role as the regional center for government and services, helps to stabilize seasonal employment during the non-fishing months (USACE, 2009).

2.4 GEOLOGIC SETTING

As reported by the USGS (**Figures 6 & 7**), bedrock exposures north of Dillingham consist of granitic rocks of Tertiary and Cretaceousage (Beikman, 1974). The depth to bedrock and its thickness are not known. The surficial geologic materials in the vicinity of the Dillingham are generally well-sorted Quaternary alluvial, glacial, and dune sand and silt deposits (Beikman, 1974). The alluvial and glacial deposits consist of gravels, sands, silts, and clays that extend to at least 63 m depth (Glass, 1987). The dune sands and silts are generally reworked deposits near the coast (Beikman, 1974).

DRAFT

The upland hills are mantled by a thick layer of loess blown in from unvegetated flood plains and hills adjacent to the melting glaciers and volcanic ash from the Aleutian Range. These plains of silt, sand, and gravel extend from about 20 to 25 km northwestward to the Wood River Mountains and eastward to, and beyond, the Nushagak River (Palcsak and Dorava, 1994).

As stated by (Palcsak and Dorava, 1994), five distinct soils series have been mapped in the Dillingham area (Rieger, 1965; Rieger et al., 1979). Aleknagik soils (approximately one-fourth of the total area) are commonly found on moraine hills and are generally well drained, extremely acidic soils in silty deposits overlying a gravelly substratum; Aleknagik soils are generally less than about 1 m thick. Kanakanak soils (approximately one-tenth of the total area) are generally well drained, extremely acidic, dark soils that are typically thick deposits over moraine hills near the rivers. Nushagak soils (approximately one-tenth of the total area) are very strongly acidic, silty soils, similar in composition to the Aleknagik and Kanakanak soils but poorly drained. These soils are generally frozen until midsummer, but permafrost does not develop in them. The water table is close to the surface (Palcsak and Dorava, 1994). Nushagak soils occupy the lower slopes of moraine hills and ridges. A few small areas of Hyer soils are found on steep, north-facing slopes. These soils, which consist largely of poorly drained organic matter and peat are perennially frozen at depths below about 40 to 80 cm. Salamatof soils are the dominant soils in the Dillingham area (slightly more than half of the total area) and occupy nearly all the low-lying areas. Salamatof soils consist of deep peat layers and muskegs and are generally more than 1 m thick. These soils are wet and are associated with many small lakes and ponds. Salamatof soils are generally frozen until midsummer, but permafrost does not develop in them. A detailed description of representative profiles of the soil series is given by Rieger (1965) and Rieger and others (1979).

The Dillingham area is underlain by isolated masses of permafrost (Ferrians, 1965), which where present, generally are at considerable depth and have been reported to be more than 50 m thick (Hartman and Johnson, 1984). Permeability of the uncompacted materials of the Aleknagik and Kanakanak soils ranges from about 2.0 to 6.4 cm/h. The gravelly material underlying the Alegnagik soils and, at greater depths, the Kanakanak soils, is more permeable than either soil type (Rieger, 1965).

DRAFT

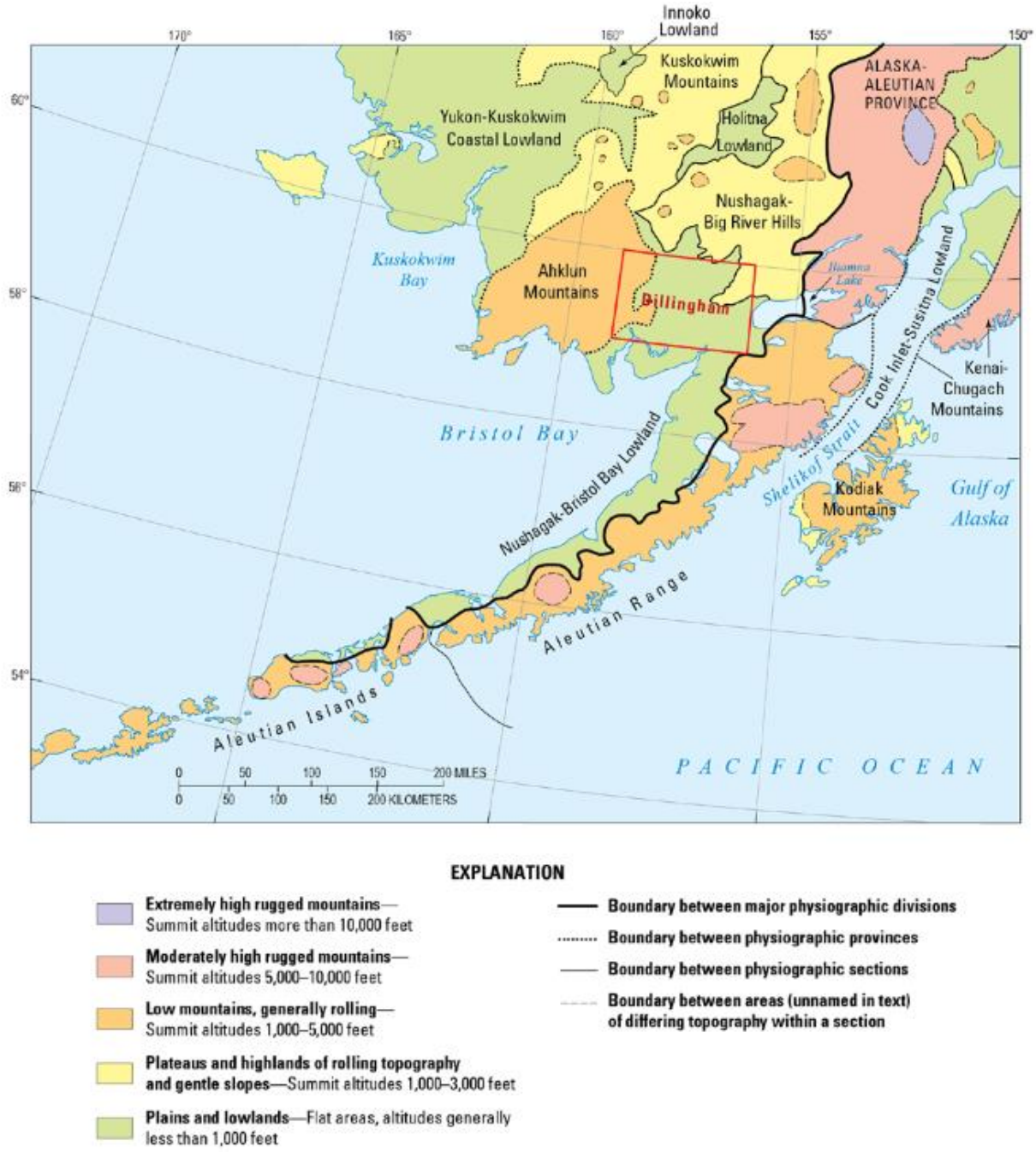


Figure 6. Physiographic provinces of southwestern Alaska after Wahrhaftig (1965). Dillingham quadrangle outlined in red. The Ahklun Mountains province covers the western part of the quadrangle. Glaciers from the Alaska Range (Southern Part) division and the Ahklun Mountains province advanced into the map area during the Pleistocene. The Pacific Mountains division of Wahrhafting (1965) is east of the heavy black line; the Intermontane Plateaus division is west of the line. The Western Alaska province (not labeled) includes the Nushagak-Bristol Bay Lowland, Nushagak-Big River Hills, Holitna Lowland, and Kuskokwim Mountains sections (from Wilson, 2018).

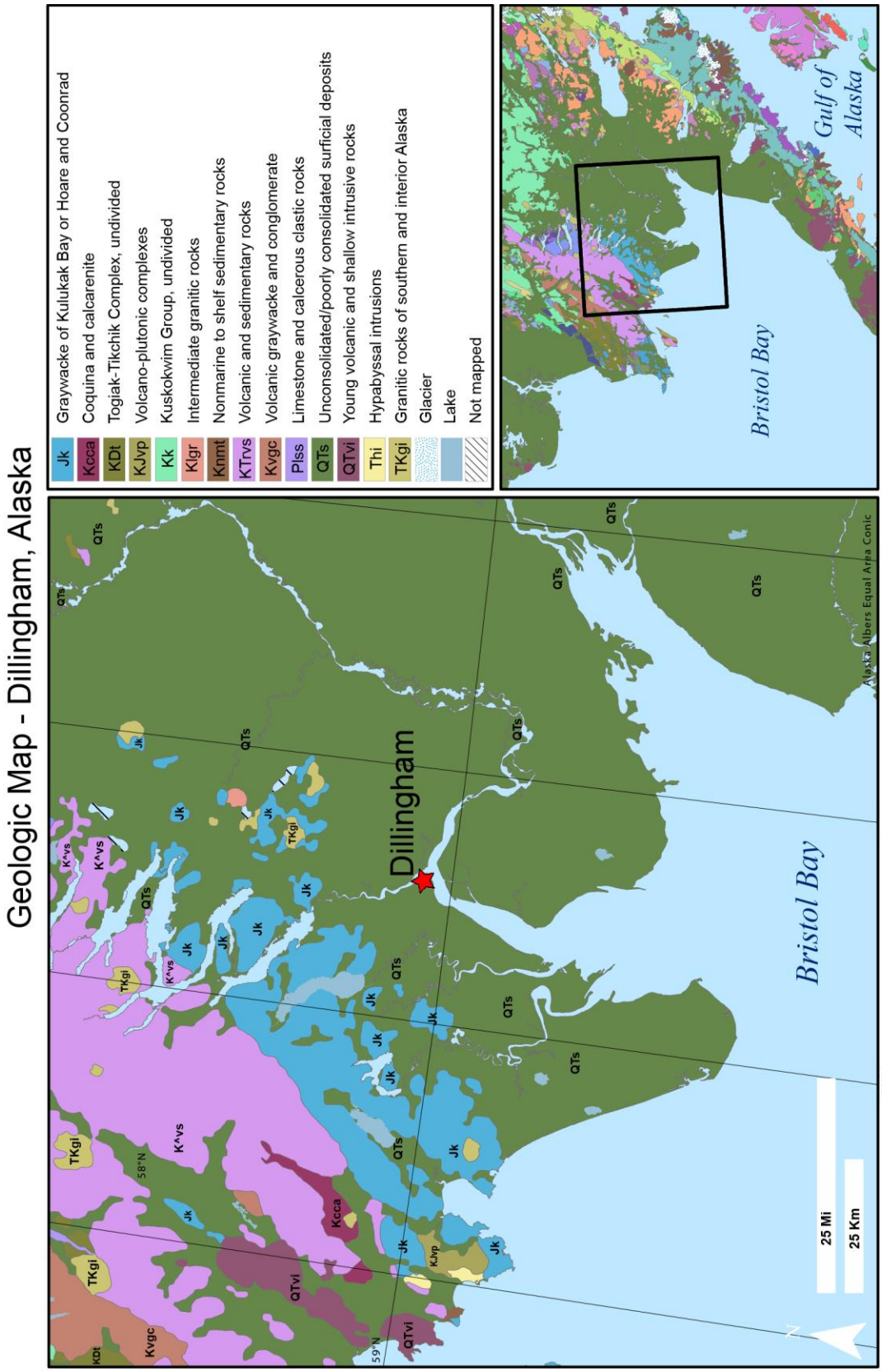


Figure 7. Generalized surficial geology of the Dillingham area (red star). Each color represents a different type or age of rock, from USGS Scientific Investigations Map 3340 - Geologic map of Alaska. Credit: Frederic Wilson and Keith Labay, USGS. Public domain. (URL: https://doi.org/10.3133/gip168).

2.5 CLIMATE AND METEOROLOGY

2.5.1 Temperature Regime

Temperatures across Alaska have increased between 1970 and 2019. Southwestern Alaska and the Aleutian Island chain have observed temperature increases of between 2 and 5 °F over this period which could have significant ecological and physical impacts (**Figures 8 & 9**). Annual temperature increases could negatively affect permafrost, sea ice accumulation, water cycling, and habitat suitability for plant and animal life. These effects could leave communities more vulnerable to coastal erosion and geomorphic hazards as a result of decreased sea ice accumulation and thawing permafrost. In addition, important subsistence food sources could be depleted by ecological changes. Fall temperatures are significant with regard to coastal erosion specifically, as higher fall temperatures decrease sea ice formation. Fall temperatures have increased less significantly than annual temperatures, but this increase is large enough to affect sea ice formation, leaving this region more vulnerable to coastal erosion (**Figures 10 & 11**).

As reported in a 1994 report by the USGS, Dillingham is in the transitional climate zone and is influenced primarily by maritime climate from early spring to late fall and to a lesser extent by the continental climate of interior Alaska from late fall to early spring (Hartman and Johnson, 1984). Conditions are commonly cool and humid with cloudy skies and moderately heavy precipitation. Strong winds and fog are not unusual (Alaska Department of Community and Regional Affairs, 1982). Fog is most prevalent in summer when moisture-laden air is warmer than the sea. Heavy fog (when visibility is reduced to 400 m) is most common during July and August. High-velocity winds, averaging 40 to 60 km/h, can continue for days or weeks at a time. Winds of about 95 to 115 km/h are not uncommon during December through March (Alaska Department of Community and Regional Affairs, 1982). Air temperatures range from a mean monthly maximum of 17.7 °C in July to a mean monthly minimum of -12.9 °C in December; mean annual temperature is 1.2 °C. Mean annual precipitation is about 640 mm; most rain falls from July through September. On average, approximately 1,850 mm of snow falls annually. Nushagak Bay is commonly ice covered from September through April of each year (Palcsak and Dorava, 1994).

DRAFT

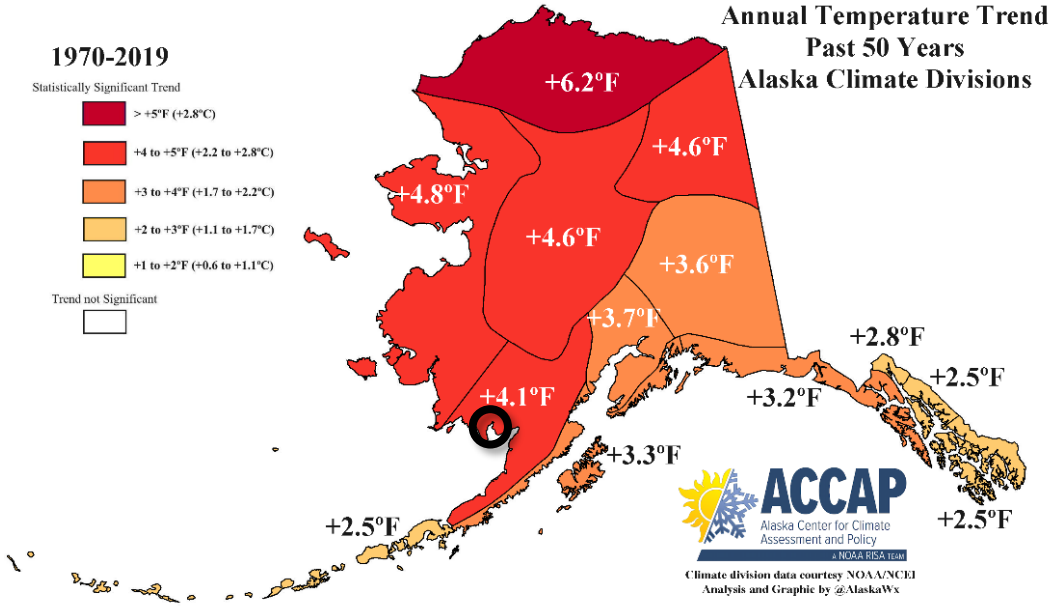


Figure 8. Annual temperature increase in Alaska between 1970 and 2019. Dillingham is in an area with a temperature increase of 2.3°C (4.1°F). Dillingham noted by black circle. Visualization courtesy of Rick Thoman and ACCAP (URL: https://uaf-accap.org/air-temperature/).

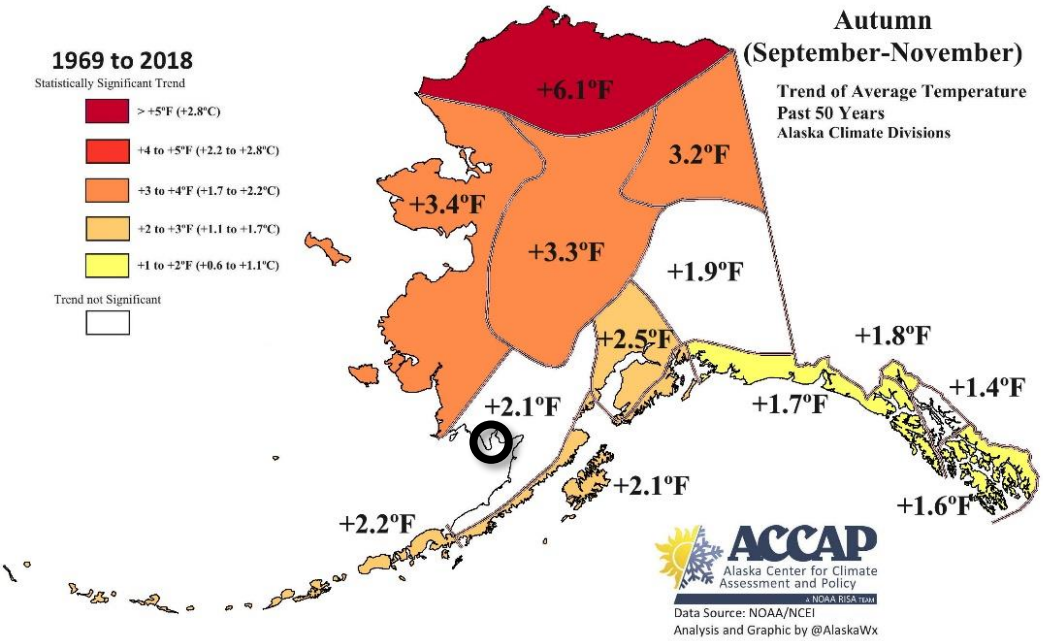


Figure 9. Autumn temperature increase in Alaska between 1969 and 2018. Dillingham is in an area with a temperature increase of 1.2°C (2.1°F). Dillingham noted by black circle. Visualization courtesy of Rick Thoman and ACCAP (URL: https://uaf-accap.org/air-temperature/).

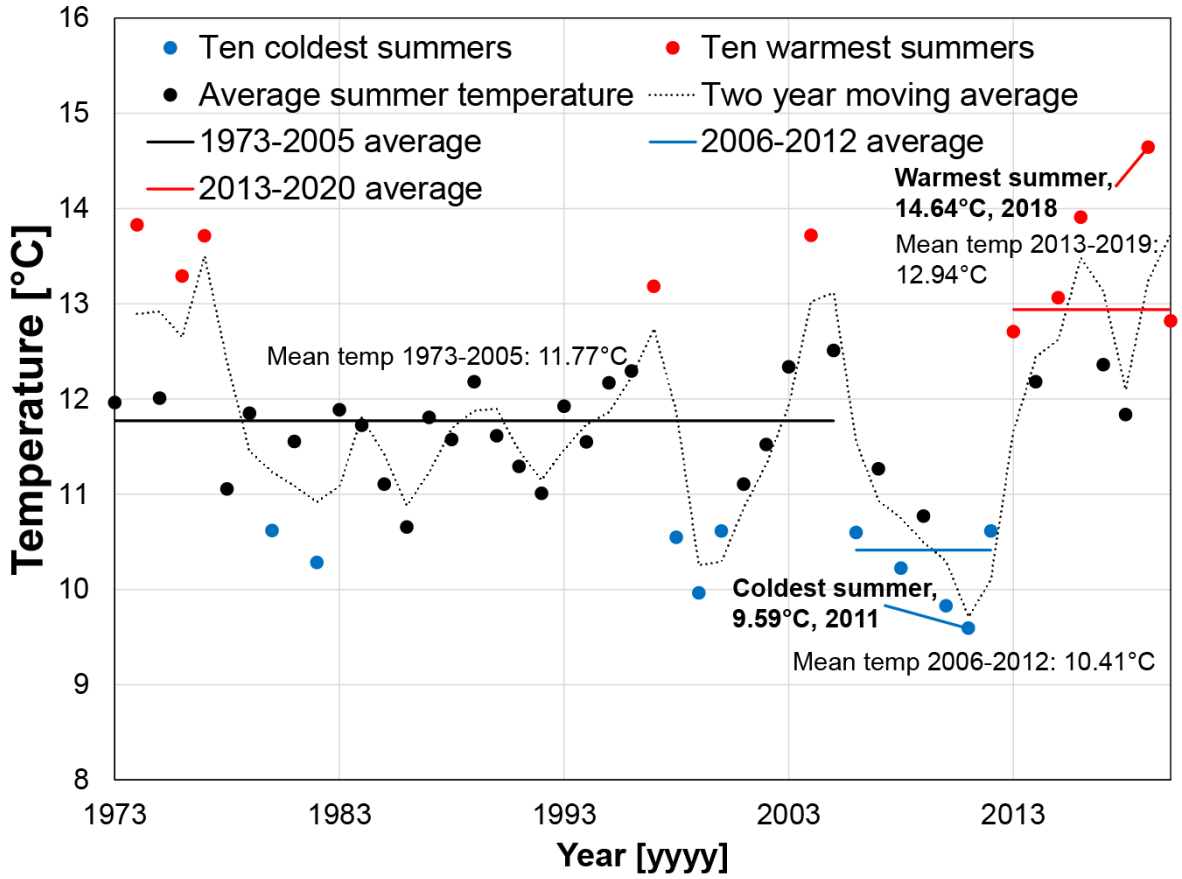


Figure 10. Mean summer temperatures in Dillingham between 1973 and 2019 based on a local airport temperature gauge. Temperature averages were calculated by taking the average of daily temperatures between June 1st and August 31st. Daily and seasonal temperature averages were calculated from the ASOS (URL: https://mesonet.agron.iastate.edu/request/download.phtml?network=AK_ASOS).

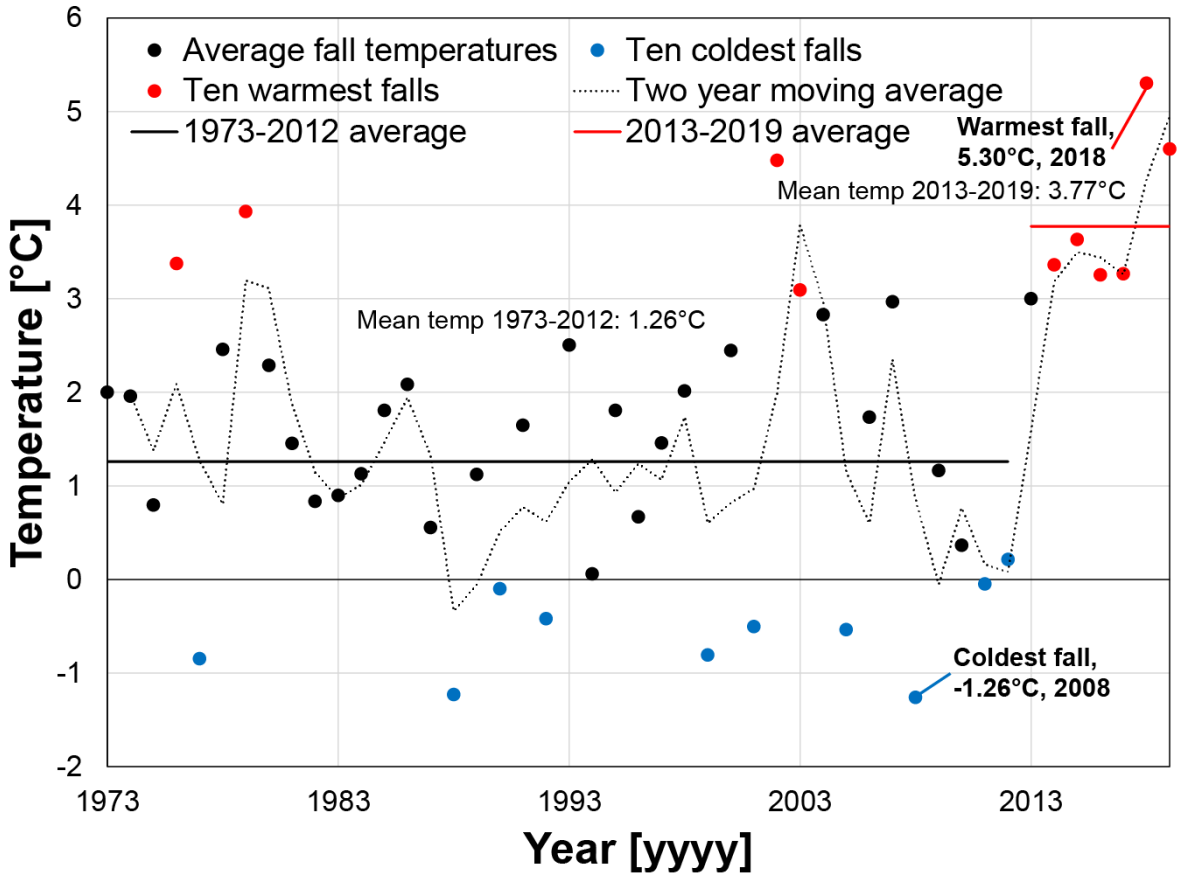


Figure 11. Mean fall temperatures in Dillingham between 1973 and 2019 based on local airport temperature gauge. Temperature averages were calculated by taking the average of daily temperatures between September 1st and November 30th. Daily and seasonal temperature averages were calculated from the ASOS (URL: https://mesonet.agron.iastate.edu/request/download.phtml?network=AK_ASOS).

2.5.2 Wind Regime

Records of wind strength and direction at Dillingham were compiled from ASOS via the Iowa State University Environmental Mesonet (**Figure 12**). The dataset was recorded at the Dillingham airport (SID: PADL) and spans approximately 50 years. The plotted data show that winds predominantly prevail from the north and are strongest during the winter months, whereas prevailing wind direction is more variable during the summer months.

More specifically, the windier part of the year lasts for 6.6 months, from September 26 to April 15, with average wind speeds of more than 11.5 miles per hour. The windiest month of the year in Dillingham is January, with an average hourly wind speed of 14.3 miles per hour. The calmer time of year lasts for 5.4 months, from April 15 to September 26. The calmest month of the year in Dillingham is July, with an average hourly wind speed of 8.7 miles per hour.

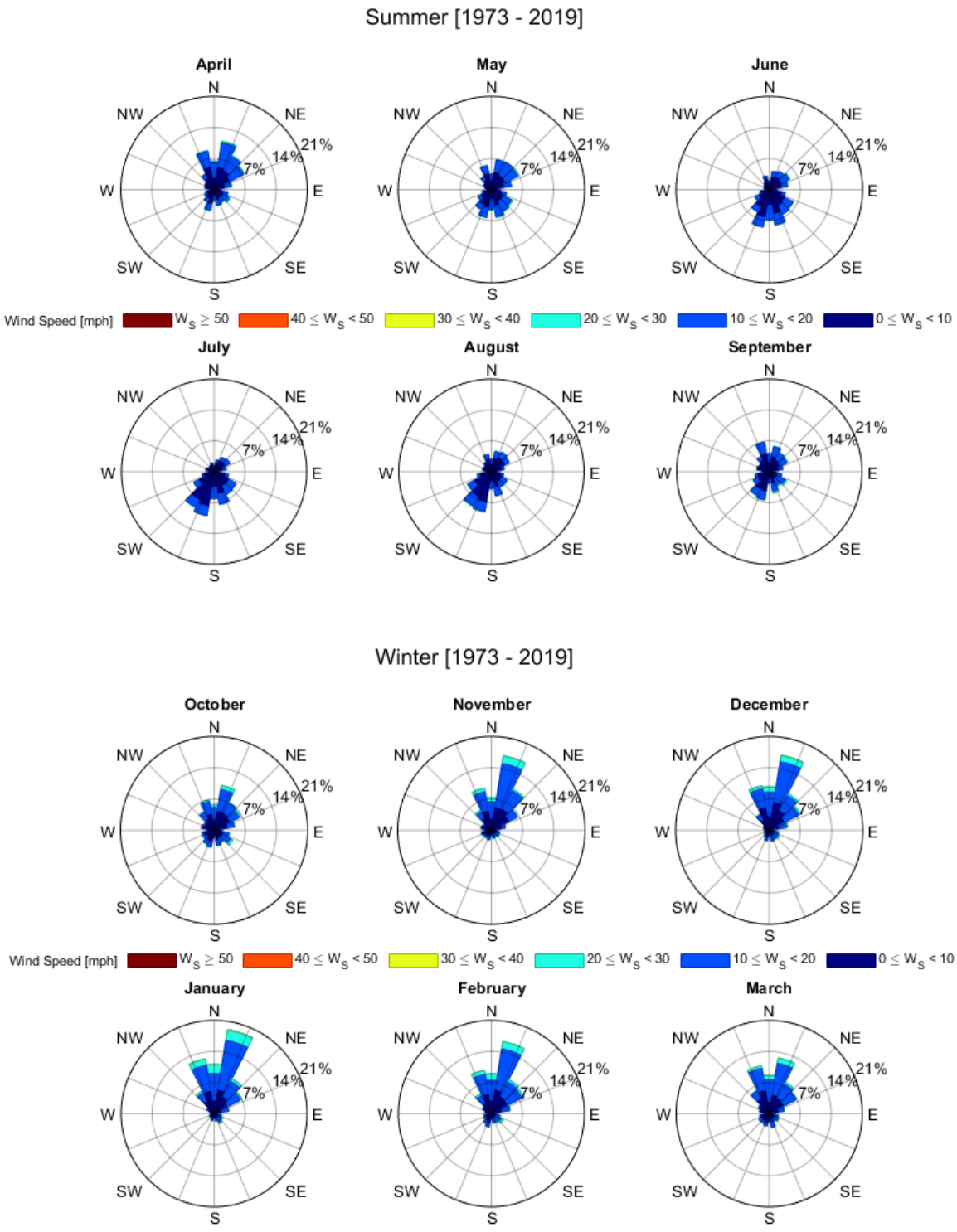


Figure 12. Averaged monthly wind roses for Dillingham (1973-2019). Spokes in each plot point in the compass direction from which winds traveled. Colors within each spoke denote wind speed bins and the length of the spokes denote the frequency of occurrence. For example, in January, 10 mph to 20 mph winds were common and prevailed from the north. (URL: https://mesonet.agron.iastate.edu/ASOS/).

2.5.3 Storm Regime

The center of a closed surface cyclonic circulation outside of the tropics is normally referred to as an extratropical cyclone (Jones et al., 2003; Bader et al., 2011). According to the Beaufort Wind Scale, an extratropical cyclone is categorized as a storm when the wind speed attains values greater than 24.5 m/s (WMO, 1970). Storms can last anywhere from 12 to 200 hours (up to >8 days), depending on the season and local geography, and can vary in size from mesoscale (≤1000 km) to synoptic scale (>1000 km). Storms are often associated with damaging winds (Mesquita et al., 2010) and/or strong precipitation in the form of rain and snow and are an integral part of the atmospheric transport of heat, moisture (Sorteberg and Walsh, 2008), and momentum polewards (Yin, 2005; Bader et al., 2011).

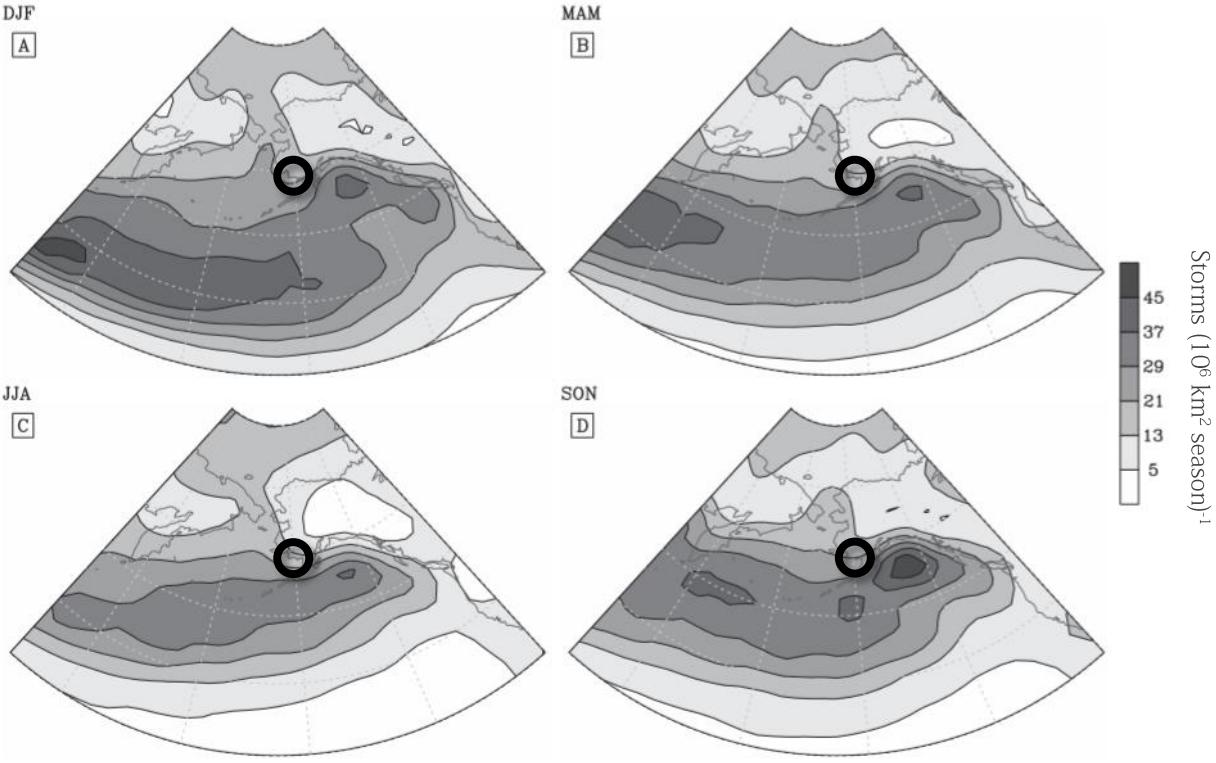


Figure 13. Storm track density climatology in the North Pacific from 1948/49 to 2008. (A) winter (DJF), (B) spring (MAM), (C) summer (JJA), and (D) autumn (SON) seasons. Units: Storms (10^6 km^2 season)$^{-1}$. Location of Dillingham is noted by the blue circles. Notice that Dillingham observes greater than 13 storms per season on average (after Mesquita et al., 2009). (URL: https://doi.org/10.1175/2009JCLI3019.1).

Understanding the trends and dynamics of coastal change in Dillingham is, ultimately, predicated on grasping both the spatial and temporal variability of storm climatologies in the North Pacific and Bering Sea (Atkinson, 2005; Rachold et al., 2005). This is because Dillingham is located in a region of substantial storm track density, especially during autumn and winter months (October – February) (**Figure 13**); with winter storms being more frequent (**Figure 13**) (Cacchione and Drake, 1979; Overland

and Pease, 1982; Sallenger et al., 1983; Mesquita et al., 2009). A study by Sepp and Jaagus (2011) found that the trend in the annual total number of cyclones in the Arctic increased by 55.8 over the period 1948–2002. There was a significant increase in the frequency of cyclones that specifically moved into the Arctic basin through the Bering Strait by Dillingham (Sepp and Jaagus, 2011). Moreover, the same study identified that the sea level pressure of Arctic cyclones showed a significant decreasing trend of 2.5 hPa (stronger storms) over the same study period.

Beach morphology and, therefore, shoreline evolution is primarily controlled by an interaction between storm frequency (surge, wave action, overwash, etc.), tidal rage, vegetation type and extent, as well as the substrate. While overwash events brought about by storm impacts may appear to be catastrophic in the short-term, they can be considered a quasi-continuous process that shapes the coastline over longer timeframes (10^2 years) (Morton et al., 2000; Donnelly et al, 2006). As such, it is all the more important to consider storm regime shifts in tandem to sea-ice dynamics as first order drivers of overwash frequency and magnitude, as well as erosion in general.

2.6 OCEANOGRAPHIC SETTING

As stated in (Palcsak and Dorava, 1994), Nushagak Bay, the northern extension of Bristol Bay, is subject to the influence of tide and wind; tidal range in Nushagak Bay is approximately 6.1 m, and the maximum significant wave with a 100-year return period is 22.5 m high (Brower et al., 1977). Dillingham is naturally protected from waves generated in Bristol Bay by the Nushagak Peninsula and by the scattered islands and mud-bar shallows in Nushagak Bay; however, the region is subject to sudden and violent storms during which locally generated waves can cause shoreline damage (FEMA, 1982).

2.6.1 Tides and Currents

In general, the tidal range increases from the mouth of Bristol Bay (~2 m) to the head (>5 m) of the bay where Dillingham is located, and local variations are heavily influenced by seasonal and interannual variability in the currents (**Figure 14**). Dillingham observes mixed semi-diurnal tides with a significant tidal range as a result of its location within the funnel-shaped embayment of the Nushagak River, which amplifies the tides (**Figures 15 & 16**). This extreme tidal range is made evident by the presence of linear shoals that are aligned parallel to the tidal currents. These shoals, approximately 10 m in height and spaced 4 km apart are characteristic of high-tidal environments.

With regards to ocean currents, the cyclonic air flow about low-pressure storm systems following the prevailing storm track in the region (southwest to northeast) causes a northward airflow along the coast such that prevailing transport currents within Bristol Bay are to the north (Hunter et al., 1979). However, there are localized micro-embayments within the Nushagak River system in which erosive eddies form because of tidal-riverine current interaction.

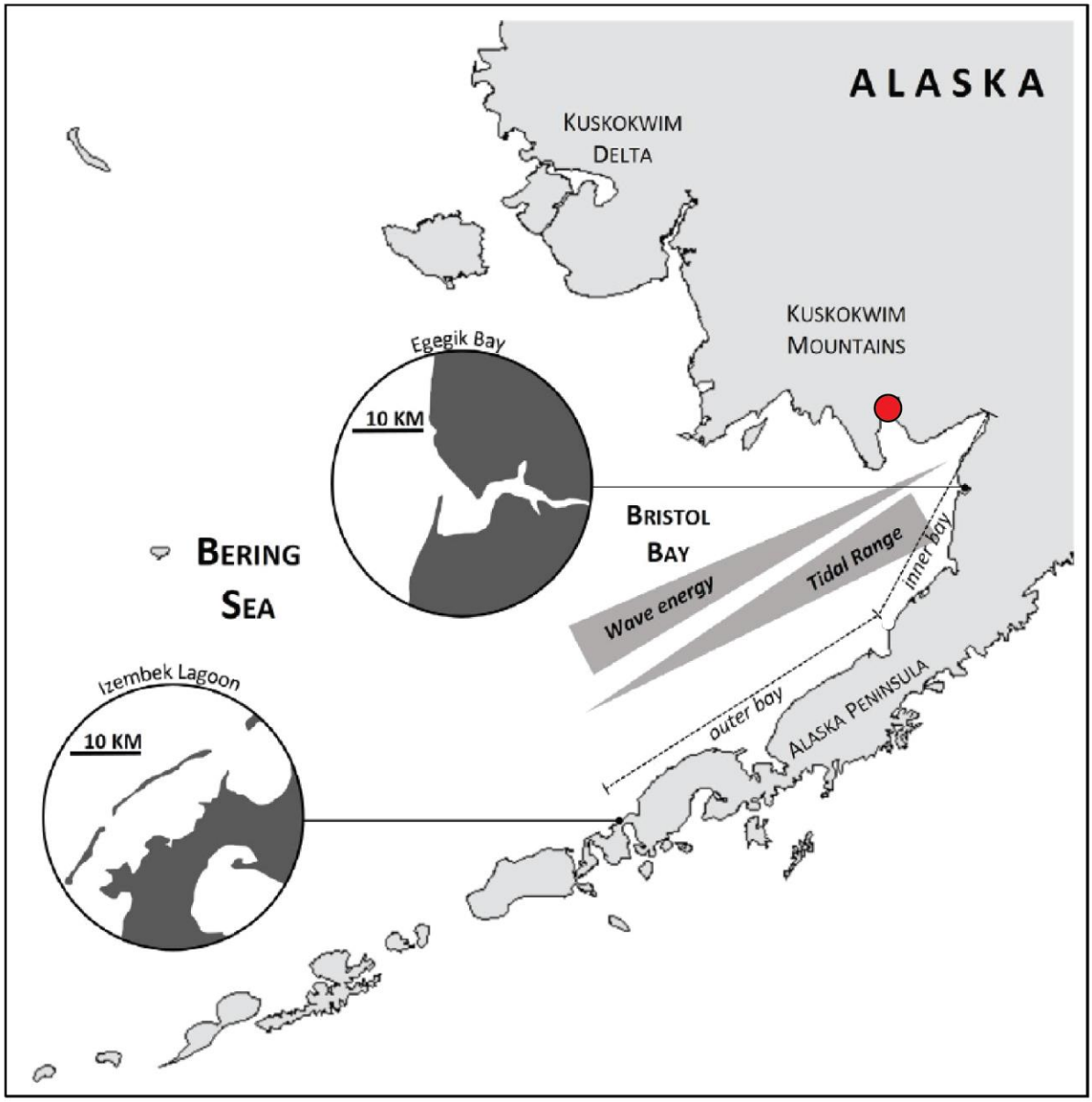


Figure 14. Graphic representation of relative strength of component marine energy (tide and wave) in Bristol Bay and the characteristic barrier morphologies in the outer (well-developed barrier islands, such as Izembek Lagoon) and inner bay (barrier spits at embayment mouths, such as Egegik Bay). Dillingham notated by the red circle (after Kinsman and Gould, 2014). (URL: https://www.arlis.org/docs/vol1/H/902693690.pdf).

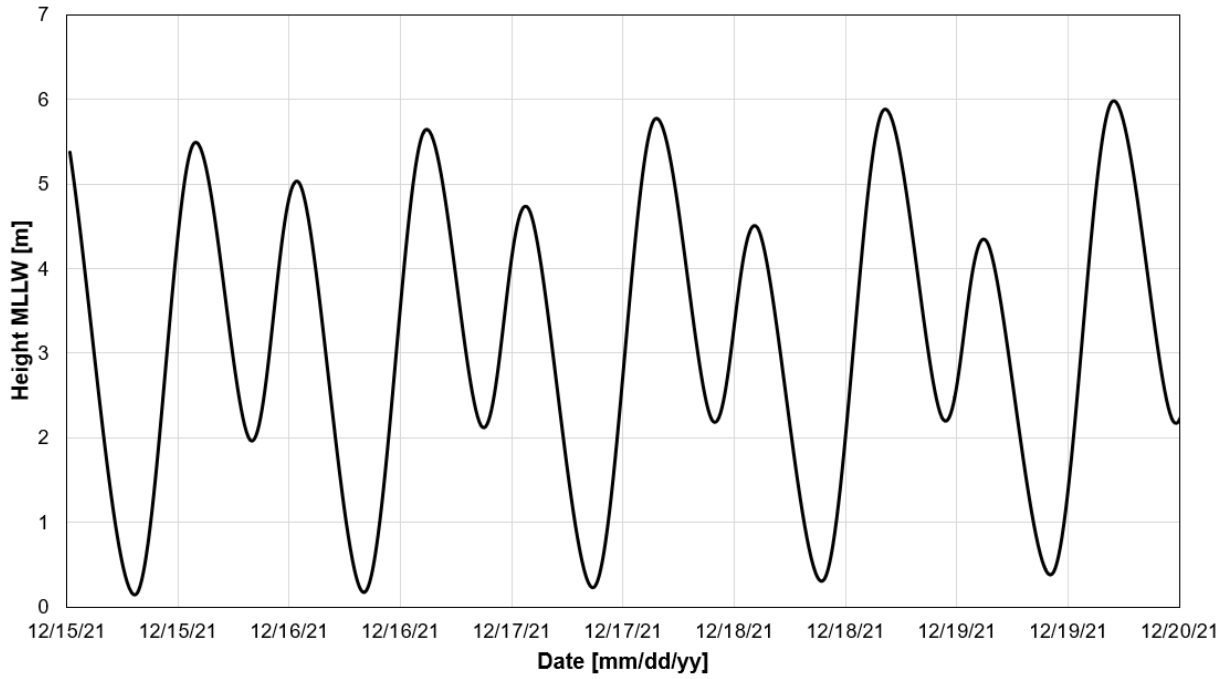


Figure 15. Example time series (12/15/21 – 12/20/21) of water level predictions from NOAA station 9465374, Snag Point, Dillingham, AK. Values represent water level height relative to Mean Lower Low Water (MLLW) in meters (m). (URL: https://tidesandcurrents.noaa.gov/stationhome.html?id=9465374).

DRAFT

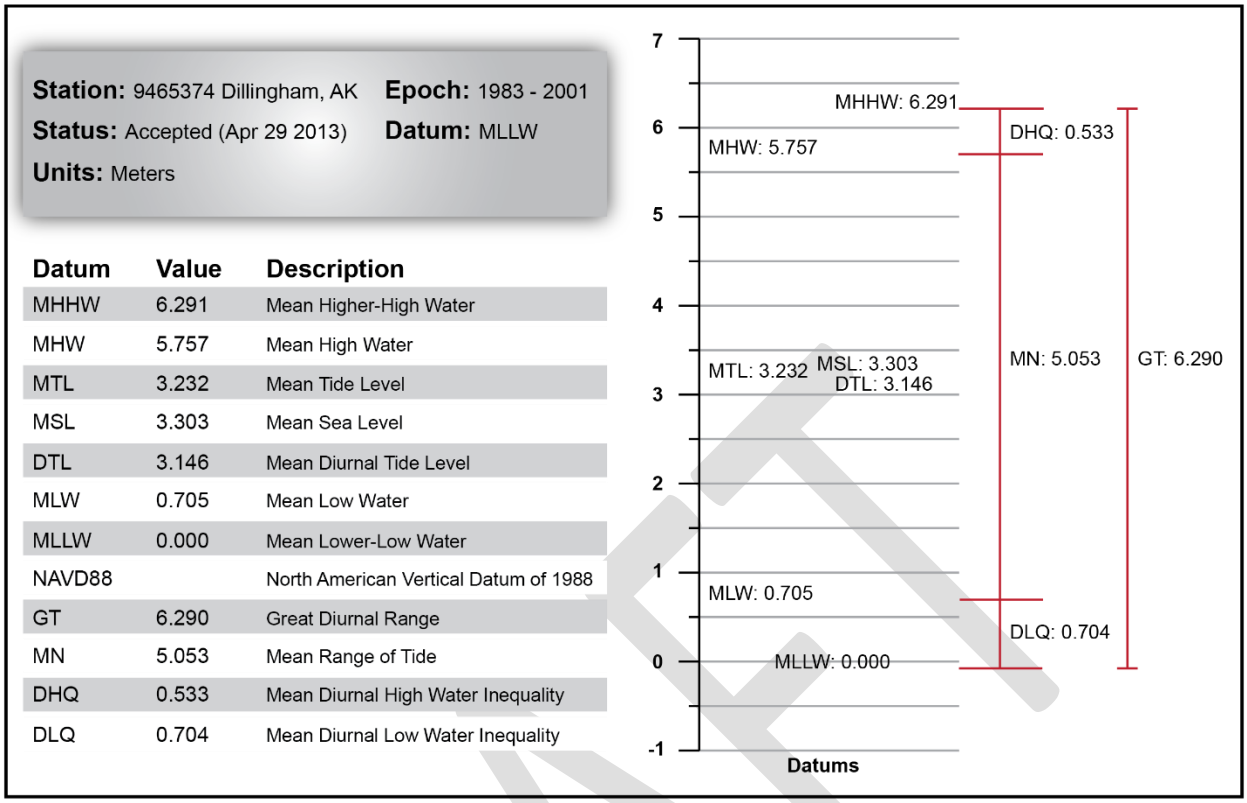


Figure 16. Tidal datum computed for Dillingham using NOAAs online data viewer. The water level gauge was vertically referenced to a land-based datum (NAVD88). (URL: https://tidesandcurrents.noaa.gov/stationhome.html?id=9465374)

2.6.2 Wave Climate

Bristol Bay is characterized by severe waves generated by local storms. Long fetch, storm duration, and shallow depth contribute to high wave conditions. In summer, when winds are from the south the nearshore Bristol Bay area is in the lee of the Alaska Peninsula. Consequently, locally generated waves are not too severe. In winter, winds are more intense and northerly. This greater fetch and speed generate increased wave heights and periods. Maximum observed heights in June are approximately 5.5 m averaging about 1.5 m. Maximum observed heights in November are approximately 9.0 m with 60% exceeding 2.0 m (Wise et al., 1987).

At Dillingham, a vast majority of erosive waves are locally generated during high wind events.

DRAFT

2.7 SEA ICE

Sea-ice extent and duration strongly influence Arctic and Subarctic coastal dynamics, and climate change is now altering the sea-ice regime of the Bering Sea (Farquharson et al., 2018). Open ocean sea-ice is an important moderator of wave fetch and water temperature, and shorefast sea-ice shields coastlines from wave action. Specifically, the extent of sea-ice has an inverse relationship with wave fetch, height, and swell size in Arctic seas (Francis et al., 2011; Overeem et al., 2011; Thomson and Rogers, 2014; Thomson et al., 2016), with the open-water season having the most wave energy available for coastal erosion and sediment transport (Overeem et al., 2011; Farquharson et al., 2018). Storms during the ice-free season generate the most geomorphologically significant wave events along Arctic coastlines and, hence, strongly influence coastal processes (Reimnitz et al., 1994; Mason et al., 1996; Forbes, 2011; Barnhart et al., 2014; Farquharson et al., 2018). Over the past three decades, there have been significant changes in the timing and extent of sea-ice cover across the Bering, Chukchi, and Beaufort Seas (**Figure 17**).

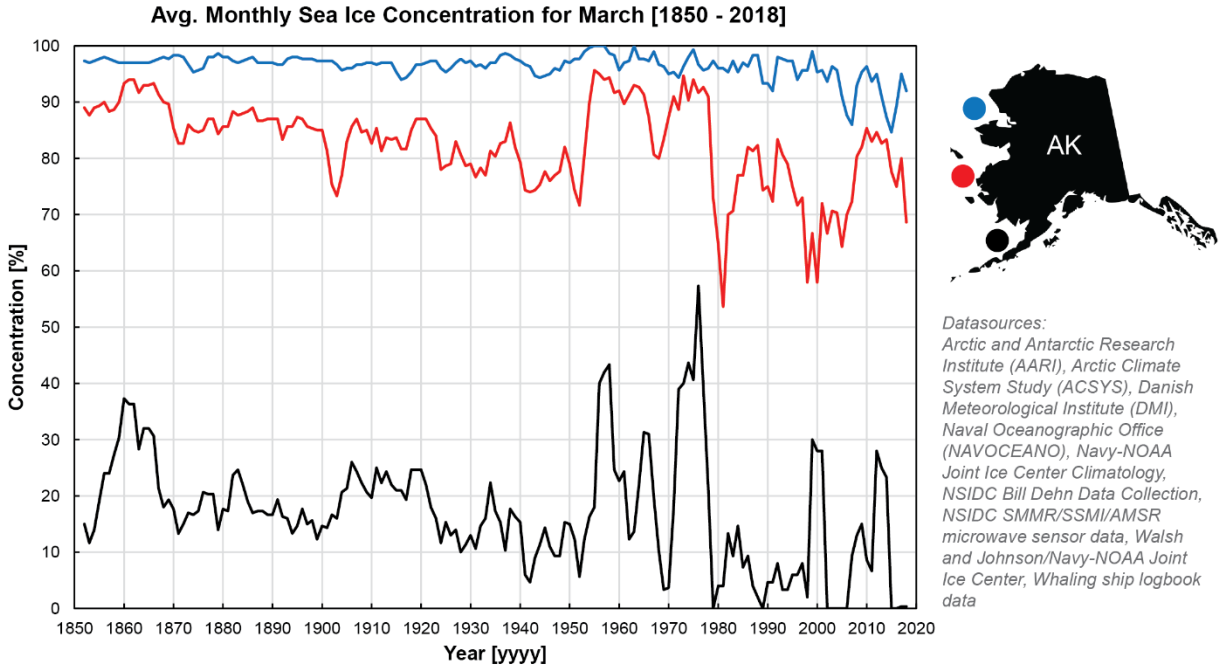


Figure 17. Sea ice concentrations for the month of March between 1850 and 2018 compiled from the Alaska Ocean Observatory Network (AOOS) Sea Ice Atlas. 0–30% indicates open water to very open drift, 30–90% characterizes open drift to close pack, and 90–100% corresponds with very close pack to compact. The black, red, and blue points in the upper right inset map correspond to the black, red, and blue sea ice time series in the main graph. Notice that sea ice in Bristol Bay (black) is no longer consistently observed each year (2000 onward). (URL: Sea Ice Atlas: Explore (uaf.edu)).

Satellite data reveal that patterns in sea-ice cover have been spatially heterogeneous through time, with significant declines of sea-ice extent in the Chukchi and Beaufort Seas, and complex multi-year variability in the Bering Sea south of St. Lawrence Island (**Figure 17**) (Frey et al., 2015). Stabeno et al. (2012) describe this multi-year variability in sea-ice cover over the southeastern Bering Sea shelf as involving oscillations between warm years (e.g., 2001–2005) with less extensive ice (driven by weak, easterly winds) and cold years (e.g., 2007–2012) with more extensive ice (driven by cold, northerly winds).

As per the extent of continuous open ocean sea ice within Bristol Bay, it generally reaches its maxima between February and March, and spatially lies roughly halfway down the Alaska Peninsula (**Figure 18**). Though, drift ice occurs south of this boundary. With significant interannual variability, landfast and/or bench ice formation in coastal shallow waters generally begins in November as far south as the Aleutian Islands.

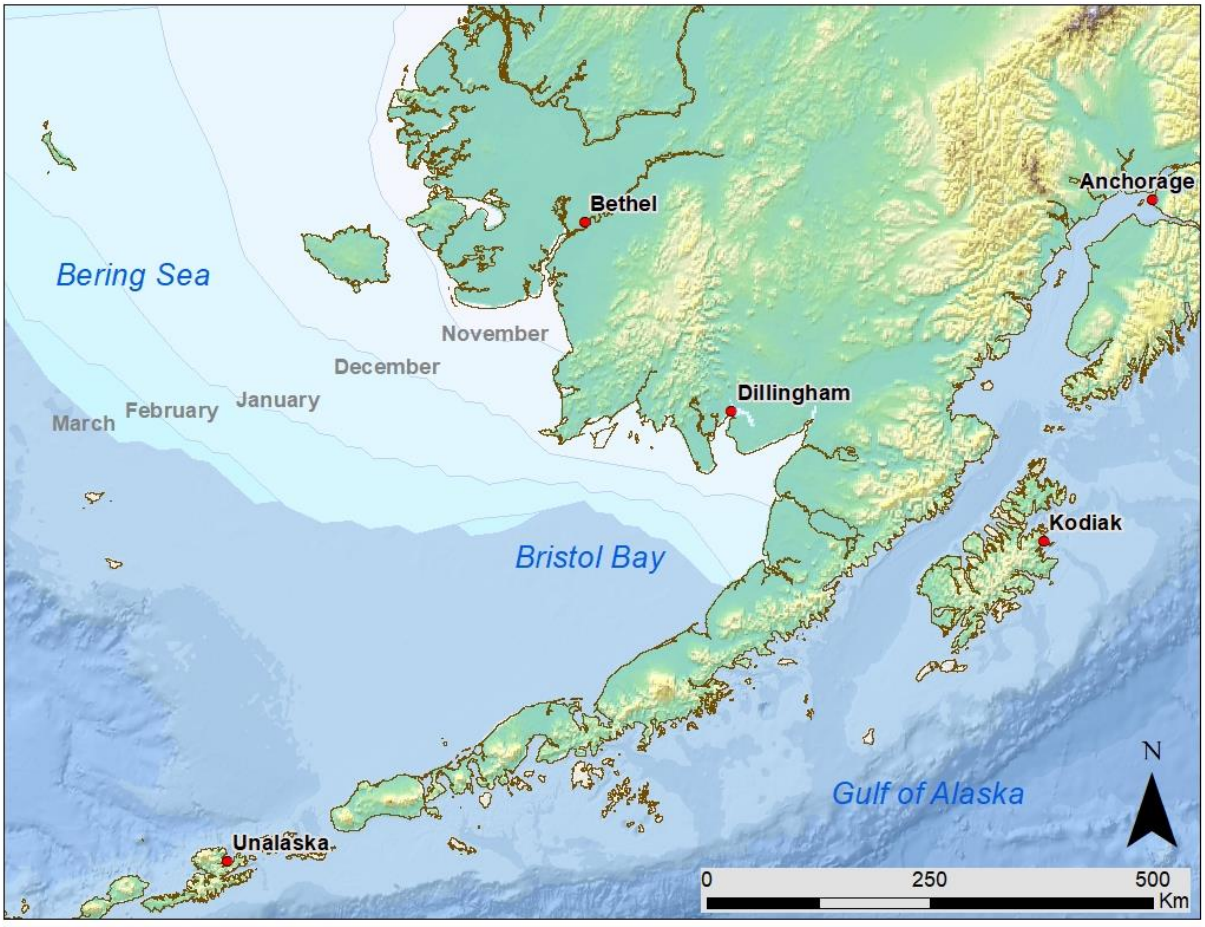


Figure 18. Average monthly sea ice extent in Bristol Bay from 1981-2010. Line data downloaded from the NSIDC and converted to polygons. (URL: https://nsidc.org/data/search/#keywords=sea+ice/).

Dillingham is ice-free from June through mid-November, though the onset of shorefast ice varies seasonally. During the sea ice season in Dillingham, ice builds up along the coast as tidal fluctuations strand ice floes and form what is referred to as bench ice (**Figure 19**). At locations where tidal flats are present, a continuous platform of landfast sea ice forms. These sea ice features serve as natural barriers against the translation of swell and wave energy on the coast (**Figure 19**). However, nearshore sea ice formation at Dillingham has trended toward a later onset and earlier break up in recent decades which equates to increased wave impact hours throughout the year (Golder Associates Inc., 2007).



Figure 19. Bench ice along the city dock. Image taken Feb, 2020.

3. NATURAL HAZARDS AND MITIGATION EFFORTS

3.1 DESCRIPTION OF HAZARDS

The following subsections (3.1.1 – 3.1.6) describe and quantify the following natural hazards: erosion, flooding, earthquakes, landslides, tsunami, and sea level change. This list specifically pertains to *coastal* related hazards and is partially based on Dillingham's FEMA-mandated hazard mitigation plan, consultation with the U.S. Geologic Survey (USGS), direct input from residents, as well as documented past occurrences.

3.1.1 Erosion

Shoreline change is the retreat or aggradation of a shoreline as a result of sediment erosion or accretion (Mangor et al., 2017). Shoreline change can occur because of changing sediment supply, oceanographic conditions, episodic storm events, terrestrial degradation through slope failure or permafrost thaw, and other nature- and human-driven processes (**Figure 20**) (Overbeck et al., 2020). Shorelines are naturally very dynamic; however, when changes occur at or near infrastructure and land used for hunting or gathering subsistence resources, erosion can be disastrous (Alaska Department of Homeland Security & Emergency Management [DHSEM], 2018).

Most communities in Bristol Bay are perched on tall (>20-ft-high) coastal bluffs as a result of the large tide range (macrotidal) and/or their proximity to river mouths (Overbeck et al., 2020). Communities located at river mouths in Bristol Bay are subject to erosion from coastal and riverine processes. The tall and exposed nature of the bluffs makes them vulnerable to groundwater seepage, overland runoff, and slumping. Coastal bluffs are fronted by mixed sand-gravel beaches, but the bluffs themselves are primarily composed of consolidated and/or clay-rich materials that are more resistant to wave impacts, compared to sandy beaches (Overbeck et al., 2020). During coastal storms, materials that slumped or were transported to the beach from the bluffs are eroded by waves. Waves can also cut niches at the base of the bluffs, which destabilizes the material above, resulting in new slumps.

DRAFT

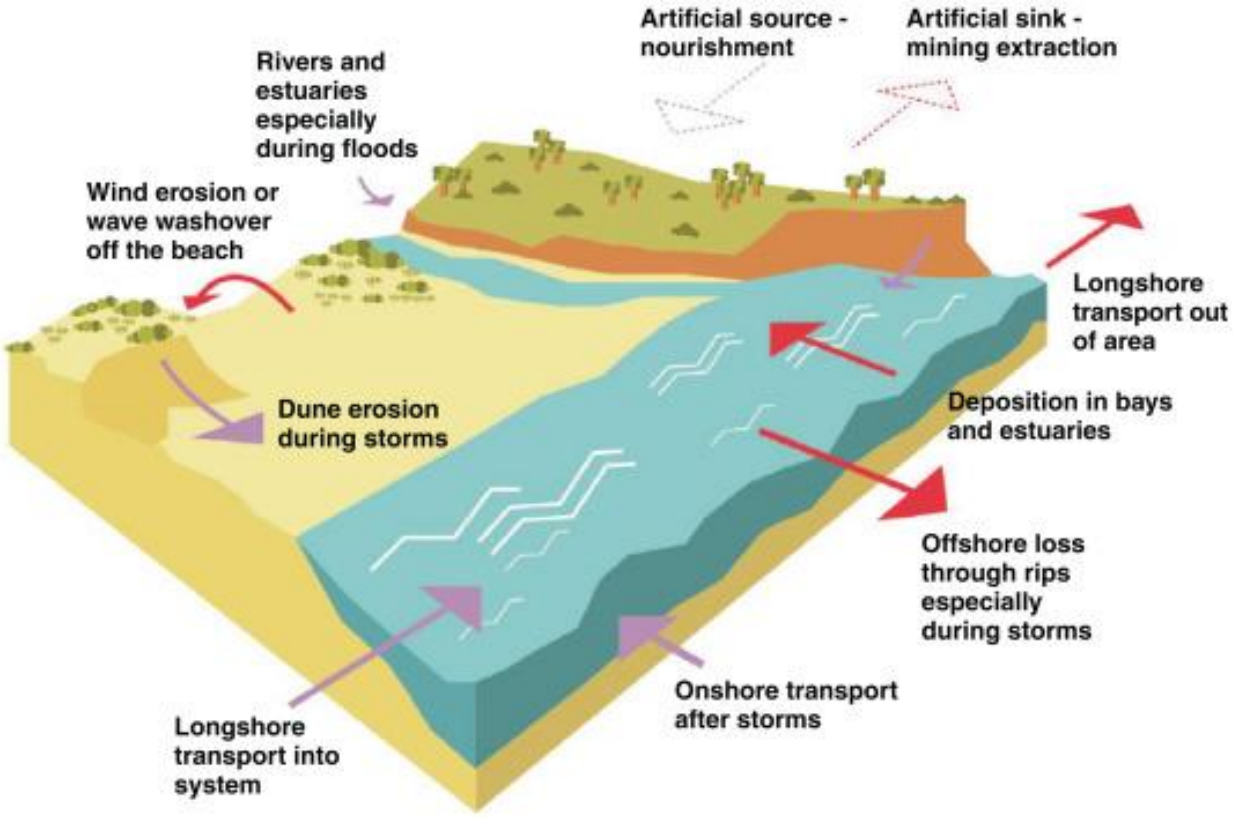


Figure 20. Components of a sediment budget for a sandy coast. From Goodwin et al., 2020 (URL: https://doi.org/10.1016/B978-0-08-102927-5.00025-4).

The City of Dillingham has experienced significant erosion loss over the past 60 years. The annual amounts of rain, wind, and waves that assail the shoreline combined with tidal fluctuations and ground water flow induce large amounts of erosion, particularly during severe storm events (Dillingham HMP, 2016). A major concern of Dillingham residents is that progressive erosion of the west bank of the city's harbor entrance has allowed wind and storm waves to have increased direct access into the harbor, causing damage to boats and harbor facilities. The City Dock Side has been eroded so severely that the picnic pavilion's foundation and trees from the city park have been washed away (**Figure 21**). Loss of the city park is a concern to locals because it is the only waterfront park area in the city. In addition, this area is also used as parking for the harbor, which is important for loading and offloading vessels, performing maintenance, and other routine small boat harbor activities.



Figure 21. City Dock Side erosion at the park. Source: USACE, 2009.

The highest rates of erosion within Dillingham are along the Wood River, adjacent to the Sewer Lagoon (**Figure 22**). This stretch of coastline has eroded approximately 20 m in only 5 years, directly threating the sewage lagoon facilities.



Figure 22. Erosion at the city sewage lagoon. Notice the actively eroding coastline. Image taken May, 2021.

Another location that is threatened from significant erosion is the Kanakanak Hospital. The hospital's sewage lagoon is just 35 m away from a bluff edge which is eroding at approximately 2 m per year. This erosion is currently impacting cultural heritage sites and burial mounds along the coastline.

3.1.2 Flooding

Coastal flooding is predominately caused by long-term elevated water levels due to highest astronomical tides. Shorter-term water level fluctuations can either enhance or dampen these long-term water level fluctuations brought about by tides. During storms, changes in sea level occur as a result of wind stress on the water surface as well as deviations in atmospheric pressure leading to positive displacement of the water level (storm surge or set-up) or negative displacement (negative surge or set-down). For example, there is a change in sea level of about 1 cm (0.4 in) for every 1 millibar (roughly 0.1 kPa) in atmospheric pressure (Fu and Pihos, 1994). As a result, sea level responds not only to pressure changes associated with weather systems but also to seasonal changes in pressure (Davidson-Arnott et al., 2019). As such, tide levels are, on average, higher during the autumn which exacerbates storm surge and is when most communities in Alaska experience flood events (Fok, 2012).

In addition to elevated water caused by storm surge, waves can wash up over the beach causing inundation, breaching, and overwash (Sallenger, 2000). Wave run-up is the sum of wave set-up and swash uprush and is added to the water level reached as a result of tides and storm setup. Runup is a complex phenomenon that depends on the local water level (including surf beat or infragravity wave effects), the incident wave conditions (height, period, steepness, direction), and the nature of the beach or structure being run-up (e.g., slope, reflectivity, height, permeability, roughness) (Dean et al., 2005; Weaver, 2008).

As such, total water level (TWL) is a summation of the processes discussed above (Erikson et al., 2018) and can be generalized as the combination of 1) a static (or assumed static or slowly varying) mean water level associated with astronomical tides, storm surges, and wave setup; and 2) a fluctuation about that mean (swash) associated with surf beat and the motion of individual waves at the shoreline (**Figure 23**). Wave run-up can add meters to the total water level on the open ocean coast, which is not only very important for inundation levels but also controls the elevation of the primary dune toe and wave impact hours as computed from a TWL time series (Ruggiero et al., 2001; Ruggiero, 2004).

DRAFT

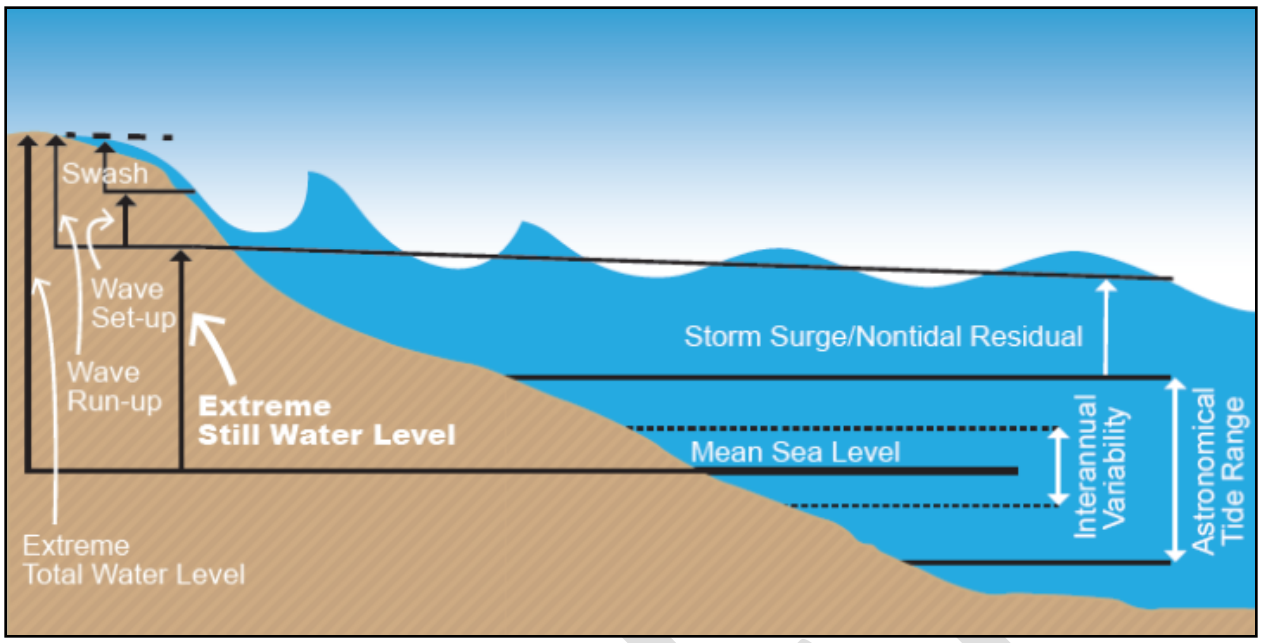


Figure 23. Diagram showing the various components of Total Water Level (TWL); waves, tides, and nontidal residuals. After Moritz et al., 2015.

Three flood types occur in the City of Dillingham:

1. Riverine flooding (also known as overbank flooding), due to excessive rainfall and minor ice-jams,
2. Coastal flooding due to wave run-up; and combination of snowmelt and rain on top of frozen ground,
3. Storm surge in conjunction with high tides and strong winds can cause significant wave run-up.

Flood boundaries have been identified by the U.S. Corps of Engineers (Alaska Department of Community and Regional Affairs, 1982) as well as the engineering firm AECOM (**Figure 24**).

DRAFT

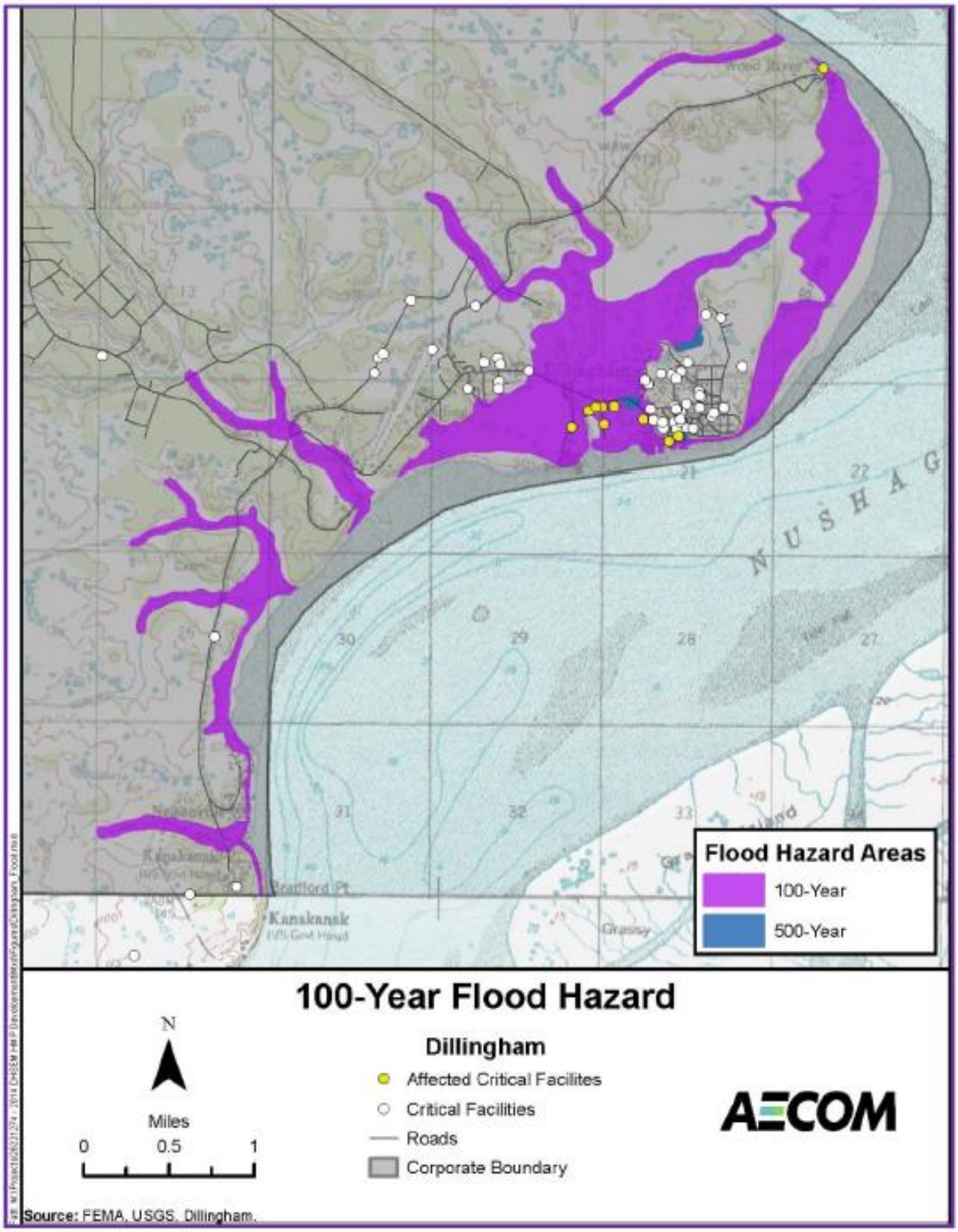


Figure 24. City of Dillingham's Identified Flood Areas by AECOM. Source: Dillingham 2016 Hazard Mitigation Report.

Flooding of Nushagak and Wood Rivers occurs in late summer or early fall from a combination of high tides and strong storm-winds from the south and southwest. More forceful storms may occur in the winter months; however, Nushagak Bay is ice covered and resistant to wave buildup from September through April of each year (FEMA, 1982). Extreme ice jamming is a remote possibility and has not been known to happen (Alaska State Housing Authority, 1971).

In general, the lowlands (wetlands and muskeg) immediately west and southwest of the townsite are the primary areas in Dillingham where flood potential is significant (Alaska State Housing Authority, 1971; Tryck, Nyman and Hayes, 1985). Where development has taken place in flood-hazard areas, it has generally been limited to the tidal waterfront, the area adjacent to Scandinavian Creek, and to a minor extent, the area adjacent to Squaw Creek (FEMA, 1982). For example, the city harbor flooded in August, 2005, resulting in damage to marine vessels and private vehicles (**Figure 25**).



Figure 25. Dillingham Harbor during a storm in August 2005. Source: USACE, 2009

Minor and highly localized flooding has occurred around creeks within the city as a result of blocked culverts and/or beaver dams, particularly in times of high run off. Additionally, very high tides frequently combine with onshore winds to temporary flood low-lying portions of the main road, impeding traffic (Dillingham HMP, 2016).

A table of documented flood events is provided below (**Table 2**). This table includes significant flood events that were documented and in no way represents a comprehensive list of every instance of flooding in Dillingham.

Table 2. Table of documented flooding events in Dillingham. Previous flood events are likely, but data on these events does not exist.

Date	Impacts
Nov 1929	Flooding did little damage, but vessels anchored in Wood River were blown up onto the flooded flats to the northeast where they remained stranded.
1962	Storms also damaged anchored vessels, leading to development of the small boat harbor on Scandinavian Creek
1980	Severe erosion and damage to the municipal dock and cold storage facilities
1993	Severe damage to Snag Point and eroded the bluff there, exposing portions of the city's sewer system, including a manhole
Aug 2005	heavily damaged Peter Pan Cannery docks and significantly eroded unprotected portions of the harbor entrance. Waves breaking over seawalls damaged vehicles parked at the harbor and moved a small building at the Bristol-Alliance fuel farm. Waves also caused minor erosion at the Delta Western and Bristol Alliance fuel facilities. The surge briefly flooded the Bristol-Alliance tank farm access road and parking lot, as well as parts of the harbor parking lot with up to two feet of water.
Feb 2009	N/A
Aug 2018	N/A

3.1.3 Earthquakes

The USGS produces probabilistic seismic hazard maps based on earthquake history and seismic potential based on the location, depth, and characteristics of geologic faults (Wesson et al., 2007). These maps indicate the probability of an earthquake event exceeding a certain measure of ground acceleration, which correlates with the most intense shaking experienced during an earthquake event. The USGS standardizes acceleration into three measures: peak ground acceleration (PGA), 0.2 second spectral acceleration (SA), and 1.0 second SA. Each of these is measured in %g, or percent of the force of gravity. PGA measures particle movement at ground level, whereas SA describes the maximum acceleration in an earthquake on an object – specifically a damped, harmonic oscillator moving in one dimension. 0.2-0.6 second SA is applicable to buildings with less than seven stories. As such, we utilize PGA and 0.2 second SA.

The probability of exceedance displayed in these maps indicates that at any given location, there is a 2% chance that an earthquake larger than the value depicted on the map occurs in the next 50 years. In Dillingham, there is a 2% chance that an earthquake with the following characteristics occurs in the next 50 years: PGA of 47%-61%g, and 0.2 second SA of 64%-85%g (**Figure 26**).

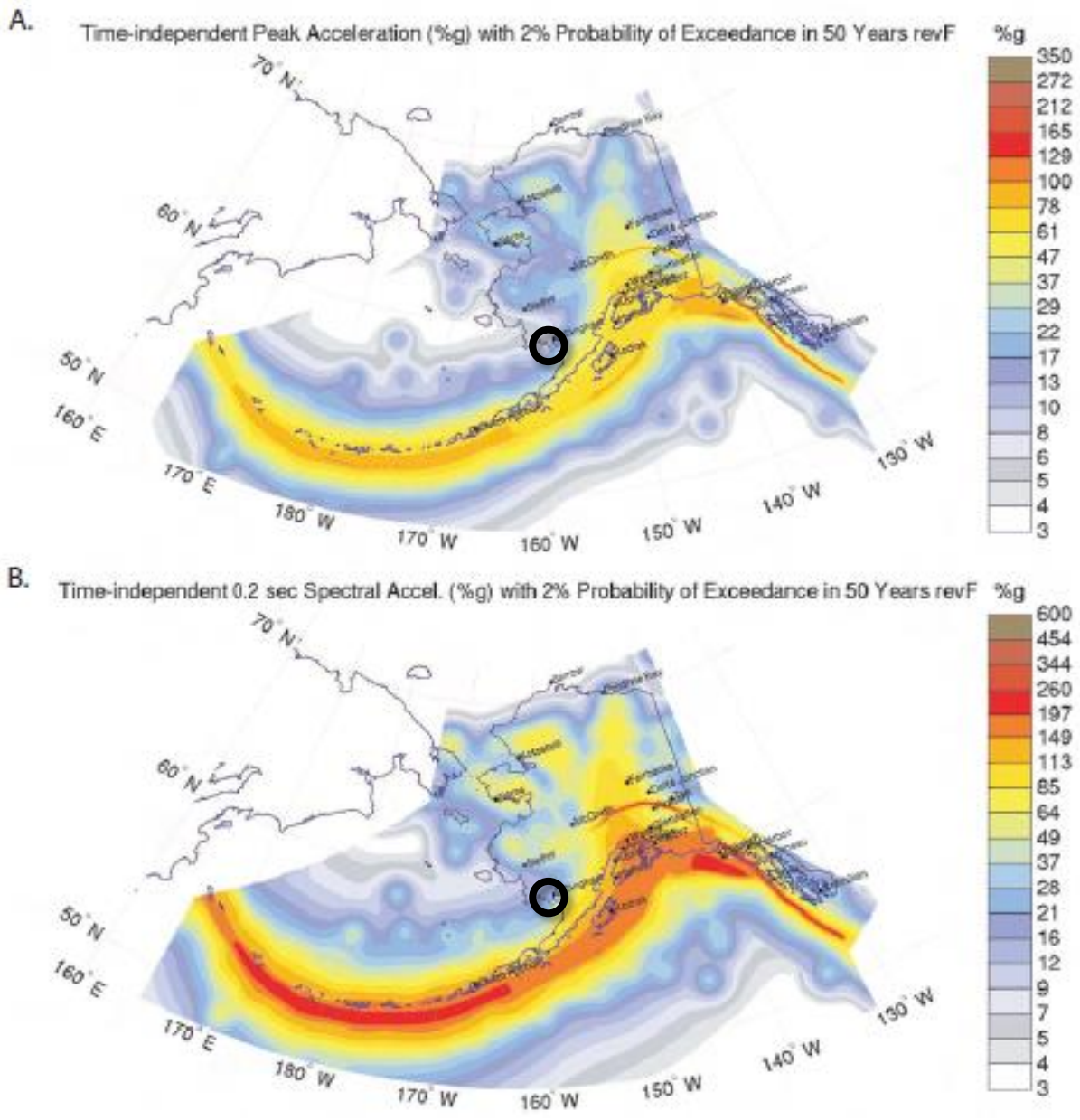


Figure 26. Earthquake probability in Alaska . Probabilistic ground motion with a 2-percent probability of exceedance in 50 years for peak ground acceleration (A), 0.2 second spectral acceleration (B). Dillingham noted by black circle. (URL: https://www.usgs.gov/natural-hazards/earthquake-hazards/hazards).

3.1.4 Landslides

There are no known landslide geohazards at Dillingham.

3.1.5. Tsunami

Dillingham is shielded from most tsunamis by the Alaska Peninsula and Aleutian Island Chain, as most seismic activity occurs on the southeast side of the island chain; however, tsunami risk remains a threat. Tsunamis within Bristol Bay are likely to come from one of three sources: underwater landslides, transpacific tsunamis, or volcanic eruptions (Suleimani et al., 2020). In 2020, the DGGS conducted a tsunami hazard assessment and determined that during severe tectonic scenarios Dillingham the maximum assumed runup height above mean highest high water (MHHW) is 1.4m (11.5ft.; **Figure 27**; Suleimani et al., 2020).

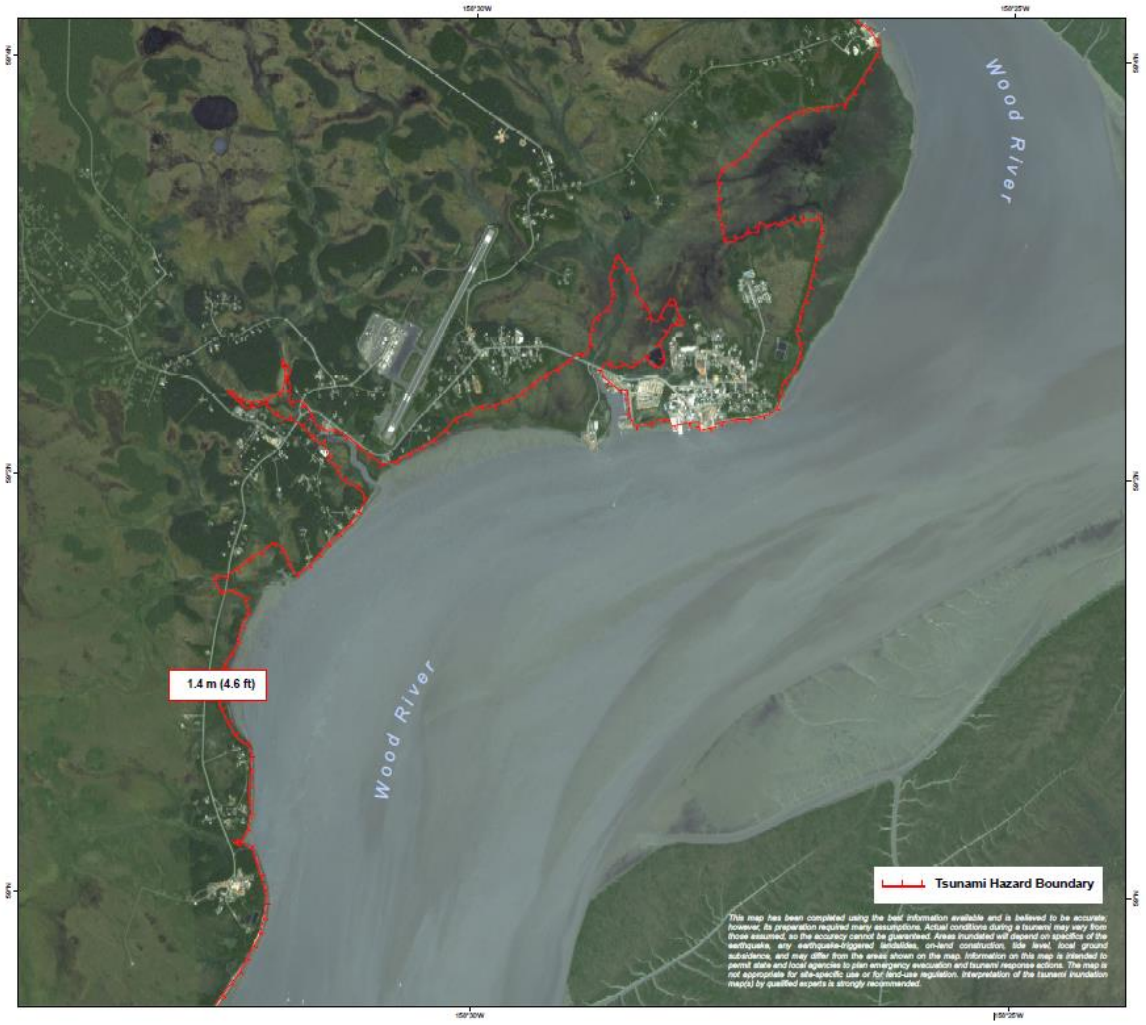


Figure 27. Tsunami hazard map of Dillingham, produced by the Alaska Earthquake Center for the Alaska Division of Geological and Geophysical Surveys (from Suleimani et al., 2020). Information on this map is intended to permit state and local agencies to plan emergency evacuation and tsunami response actions. The map is not appropriate for site-specific use or for land-use regulation. (URL: https://dggs.alaska.gov/webpubs/dggs/ri/oversized/ri2020_001_sh003.pdf).

3.1.6 Sea Level Change

A large number of studies worldwide suggest that over the past 1,000 years global average (eustatic) sea level has risen at a rate of <2mm (<0.08 in) per year (Gornitz, 1995). Eustatic sea level has risen about 21–24 cm (8–9 in) since 1880, with about a third of that occurring in the last 25 years. The rising water level is mostly due to a combination of meltwater from glaciers and ice sheets and thermal expansion of seawater as it warms. In 2019, global mean sea level was 87.6 mm (3.4 in) above the 1993 average—the highest annual average in the satellite record (1993-present). From 2018 to 2019, global sea level rose 6.1 mm (0.24 inches) (Wuebbles et al., 2017; Cazenave et al., 2018; Davidson-Arnott et al., 2019).

Relative sea level rise (RSLR) is the combination of eustatic (global) sea level rise and local land subsidence (or in some cases, rise in land elevation) (Figure 28). This local change in land elevation has a variety of causes, such as earthquake deformation cycles, groundwater reduction or increase, oil extraction, etc. RSLR in the Dillingham area…

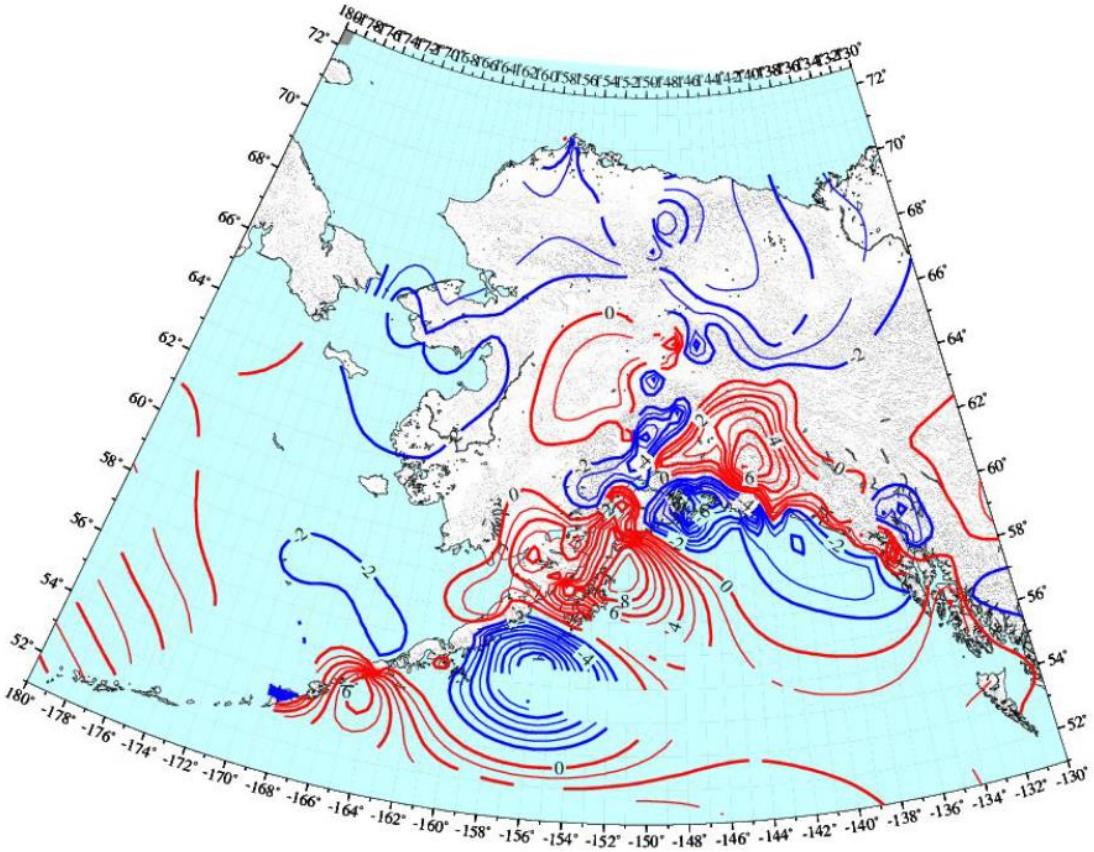


Figure 28. Predicted uplift rates with glacial isostatic adjustment subtracted, in mm/yr. This map is made by contouring vertical adjustment rates derived from various permanently operating GNSS stations across the region and subtracting signals brought about by post-glacial rebound. Contour interval is 1 mm/yr, and every other contour is labeled (from Freymueller, 2013). (URL: http://gps.alaska.edu/jeff/Snay-Freymueller-2016_GPS_velocities.html).

3.2 PAST/ONGOING MITIGATION EFFORTS

Most erosion mitigation projects have taken place in and round the city harbor as well as Snag Point. As stated in Dillingham's 2016 Hazard Mitigation Plan, previous efforts to control riverbank erosion near the small boat harbor consisted of timber plank and pile bulkheads built in 1983 by the City of Dillingham at Snag Point, about ¾ mile east of the small boat harbor; 1,600 feet of sheet-pile bulkhead built by the Corps at Snag Point between 1995 and 1998 (Dillingham HMP, 2016); and about 600 feet of sheet-pile bulkhead built by the Corps immediately east of the harbor entrance in 1999 (Dillingham HMP, 2016). In addition, Bristol Alliance Fuels has installed a sheet-pile wall to protect their mooring facilities. Erosion control efforts by the Corps to date total more than $6 million.

Other private efforts to control erosion have been attempted along the west bank of the harbor entrance channel. These efforts consisted of sheet-pile and wood bulkheads that failed to withstand the energy of storm waves, and their remains offer little or no stabilization to the shoreline in this area today.

DRAFT

4. DATA PRODUCTS AND ASSESSMENT TOOLS

This research was conducted in part to assess spatial patterns of vulnerability to erosion and flooding over long- and short-timescales, as well as to identify at-risk infrastructure in Dillingham. This was accomplished through ground-, water-, and air-based surveys coupled with computer-based processing and analysis using a geographic information system (GIS).

4.1 PREVIOUS ASSESSMENTS

Numerous studies have been done in the Dillingham area; 13 studies were done by the Corps, and at least three studies were done by others dating from 1960 to 2002 (USACE, 2009). The University of Alaska Fairbanks ACGL has been actively conducting coastal hazard related research at Dillingham since 2016 (**Table 3**). This includes a series of topographical surveys, the establishment and maintenance of erosion monitoring sites, and the collection of hydrographic datasets such as waves, water levels, and bathymetry. The results of this continuing work are delivered in this report.

DRAFT

Table 3. Summary of ACGL community visits and field work.

Date	Individuals	Research Activities	Monitoring Activities	Outreach
August 2016	Chris Maio, Richard Buzard, Gabe Dunam, Jaci Overbeck, Sue Flensberg	• UAV survey • GNSS survey	• Establish new sites	• Meeting with environmental program staff • Stakes for Stakeholders workshop
September 2017	Chris Maio, Rich Buzard, Gabe Dunam, Sue Flensberg	• UAV survey • GNSS survey	• Site maintenance	• Meeting with environmental program staff • Community meeting
August 2018	Chris Maio, Gabe Dunam, Sue Flensberg	• GNSS survey	• Site maintenance	• Meeting with environmental program staff
February 2020	Reyce Bogardus, Chris Maio, Gabe Dunam		• Site maintenance	• Meeting with environmental program staff • Community meeting • POLARIS workshop
May 2021	Reyce Bogardus, Chris Maio, Roberta Glenn, Gabe Dunam, Sue Flensberg, Renee Roque	• GNSS survey • Install wave buoy(s) • UAV survey(s)	• Site maintenance	• Meeting with environmental program staff • Community meeting
October 2021	Reyce Bogardus, Chris Maio, Matthew Balazs, Michael Letzering	• Install water level gauge • UAV Survey(s)	• Site maintenance	• Meeting with environmental program staff • Meeting with Kanakanak Hospital • Meeting with Curyung Tribe • Meeting with BBNA
June 2022 (Planned)	Reyce Bogardus, Chris Maio, Jessie Christian, Matthew Balazs, Oliver Nessel, Desi Bond, Slue Flensberg	• GNSS survey • Install wave buoy(s) • UAV survey(s)	• Site maintenance	• Meeting with environmental program staff • Meeting with Curyung Tribe • Meeting with city

DRAFT

4.2 REFERENCE DATASETS

The following subsections (4.2.1 – 4.2.5) describe baseline geospatial datasets and hydrological datums as collected or compiled by the ACGL. These data contain aerial imagery, continuous elevation surfaces, as well as discrete point data. Source information and links to data portals are included in sections related to compiled data. This information is intended to assist any future environmental assessments of Dillingham. Data collected by the ACGL is available upon request.

4.2.1 Ground Control Points and Checkpoints

Ground control points (GCPs) and checkpoints are locations on the ground that have a precise coordinate associated with them. In photogrammetry, they are used to tie the map down to the Earth—matching the drone or satellite location data to the location data measured terrestrially. It's important to note that GCPs are not the same as checkpoints, which are used in post-processing to validate accuracy by checking the map against the known points on Earth as captured during the survey.

At Dillingham, the ACGL has collected 154 GCPs or checkpoints (**Table 4**).

Precise horizontal and vertical measurements were collected with a GLONASS-enabled GNSS system consisting of dual frequency Trimble R2 and R8s receivers with a TSC3 field controller running Trimble Access software (e.g. Kinsman and DeRaps, 2012; Buzard, 2017). These measurements broadly fall into the following categories during three field surveys: ground control points and checkpoints, shoreline indicators, profiles, benchmarks, and other (including waterlines, timelapse camera locations, erosion monitoring stake locations, and water level gauges) (**Table 4**).

Table 4. Summary of GPS survey points per product type and date.

Date	GCPs	Shorelines	Profiles	Benchmarks	Other	Total
2016	0	4,021	127	2	8	**4,158**
2017	104	0	74	0	7	**185**
2018	0	2,051	120	0	1	**2,172**
2021 MAY	28	3,271	455	2	1	**3,757**
2021 OCT	22	2,109	381	0	3	**2,515**
Total	154	11,452	1,157	4	20	**12,787**

4.2.2 Benchmarks

NOAA's National Geodetic Survey (NGS) manages approximately 240,000 stations gathered over the last two centuries. This survey benchmark data is made available through the National Geodetic Survey Data Explorer (https://geodesy.noaa.gov/NGSDataExplorer/). Two main types of benchmarks exist – "vertical control points" and "horizontal control points". Vertical control points contain a precisely measured orthometric height. The elevation is usually measured as height above sea level. Horizontal control points simply contain latitude and longitude values. Within these two broad types of survey benchmarks, there are different types of categories for horizontal control markers as described in NOAA's Horizontal Control documentation. There are fourteen NGS benchmarks in and around Dillingham; ten are purely horizontal reference points (**Table 5**).

Table 5. NGS benchmarks within 10km of Dillingham

Site Name	Latitude	Longitude	Geoid Height (m)	Control Type
UV7707	N 59 00 01.23979	W 158 33 02.29746	N/A	Classic Horizontal
UV7705	N 59 00 02.31279	W 158 32 12.45382	N/A	Classic Horizontal
UV7706	N 59 00 57.88177	W 158 32 30.02035	N/A	Classic Horizontal
UV7709	N 59 03 00.38496	W 158 35 05.10564	N/A	Classic Horizontal
UV7704	N 59 02 09.74162	W 158 30 48.64834	N/A	Classic Horizontal
DN1952	N 59 02 25.75945	W 158 30 44.12023	13.286	GPS Station
UV7703	N 59 02 27.33235	W 158 30 36.38145	N/A	Classic Horizontal
UV7702	N 59 02 24.97196	W 158 30 27.20661	N/A	Classic Horizontal
DN1839	N 59 02 42.23125	W 158 30 27.74762	13.281	GPS Station
UV7701	N 59 02 44.90130	W 158 30 14.64347	N/A	Classic Horizontal
DN1953	N 59 03 22.13034	W 158 29 38.76314	13.268	GPS Horizontal
UV7690	N 59 02 24.00730	W 158 27 34.86684	N/A	Classic Horizontal
UV7691	N 59 03 43.02931	W 158 28 14.85652	13.256	GPS Station
UV7689	N 59 04 05.36728	W 158 22 15.44200	N/A	Classic Horizontal

4.2.3 Digital Surface Models and Orthomosaics

Digital surface models (DSM) of the city and hospital's sewage lagoons were derived from aerial photographs taken from Unmanned Aerial Systems (UAS) (**Figures 29 and 30**). These models were used to rectify orthomosaics of the areas and add to a series of such models starting from 2016. The DSMs and orthomosaics allow for volumetric and lateral change detection.



Figure 29. City lagoon model collected May 2021.

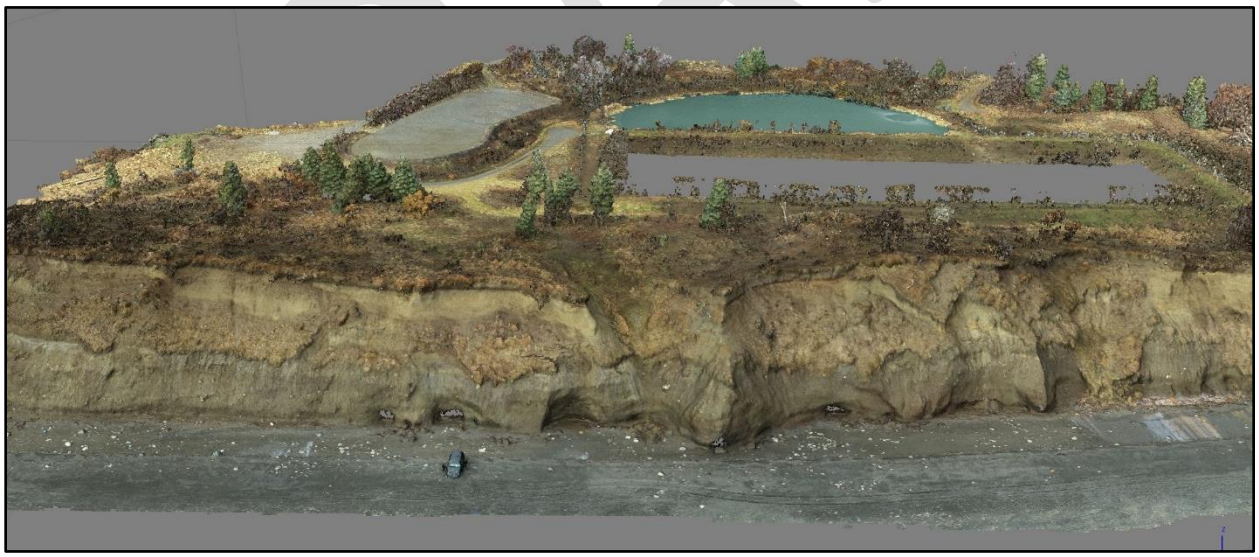


Figure 30. Hospital lagoon model collected October 2021.

The surveys were accompanied by an extensive ground control campaign using RTK-GNSS to vertically reference the DSMs (Watanabe and Kawahara, 2016), relate elevations to the tidal datum computed for this project (Antunes, 2000), but also to validate the vertical accuracy of the refined topographic surfaces (James et al., 2017). This validation was carried out following Gindraux et al. (2017), where the horizontal and vertical values of the unused GCPs from the alignment phase are compared against the refined topographic surface.

4.2.4 Tidal Datums

A tidal datum is a standard elevation defined by a certain phase of the tide and is used as a reference to measure local water levels. Tidal datums are calculated from geodetically tied local water level data, which provides a necessary conversion for storm forecasting and floodplain mapping (Overbeck, 2018).

Dillingham had a tidal datum computed first in 2012, but there have been various new water level sensors installed in and around Dillingham since then. These new instruments will allow for an updated datum to be computed.

DRAFT

4.2.5 Bathymetry

The National Centers for Environmental Information (NCEI) maintains the digital data archive for all hydrographic data of the coastal waters and exclusive economic zone of the United States and its territories collected by Coast Survey. The database provides hydrographic survey products which contain additional details of the ocean floor not shown on the nautical charts. NCEI also maintains an interactive data viewer for other sources of bathymetric and ocean depth data collected by other agencies.

This interactive viewer (https://www.ncei.noaa.gov/maps/bathymetry/) allows for the identification of NOAA bathymetric data for both visualization and download. The viewer contains single beam track lines, multibeam surveys and mosaics for data visualization, the NOS hydrographic surveys, BAG footprints and shaded imagery, digital elevation models (DEMs), and coastal LiDAR datasets available.

Dillingham has bathymetric surveys spanning more than 60 years (**Table 6**).

Table 6. Overview of compiled bathymetry surveys of Dillingham. The survey, survey type, year of acquisition, source, and datum is provided.

Survey	Type	Year	Source	Datum
H07668	Single Beam	1948	NOAA	MLLW
H07669	Single Beam	1948	NOAA	MLLW
H12398	Single Beam	2012	NOAA	MLLW
H07670	Single Beam	1950	NOAA	MLLW
H12399	Single Beam	2012	NOAA	MLLW
H12400	Single Beam	2012	NOAA	MLLW
H07769	Single Beam	1950	NOAA	MLLW
H03178	Unknown	1909	NOAA	Unknown

4.3 REPEAT DATASETS

To better understand the processes that continuously shape the landscape and quantify change, repeat measurements of the surface are needed. After the first measurements of the surface are taken (known as the baseline dataset) subsequent data collected over the same location can be compared. Each survey must be accurately co-registered to the previous data to minimize error when calculating change. This report summarizes the findings from several repeat surveys including, shoreline indicators, stake measurements, cross-shore profiles, and timelapse photography.

4.3.1 Shoreline Indicator Position

A shoreline is a linear demarcation between land and water that can represent a visual feature or an elevation contour on the beach. Either type of shoreline (i.e., visual- or elevation-identified) can be delineated within a Geographic Information System (GIS) program (e.g., ArcGIS) based on source orthoimagery or elevation data (Overbeck et al., 2020). Shoreline data are created in the form of a vector (line) that represents the shoreline position at a particular time along a section of coast. For example, if multiple shoreline datasets are available, they can be compared visually to show how the shoreline has changed through time. The distance between shoreline vectors can also be measured to compute shoreline change distances and rates. The primary remote sensing datasets utilized for this work were orthoimagery, since not only does Alaska lack high-resolution elevation data along the coastline, but also tidal datums by which shoreline features are extracted from elevation data are not well established (Overbeck et al., 2020).

At Dillingham, the linear position of the shoreline in 1952, 1980, 2001, 2006, 2011, 2016, 2018, 2021, and 2022 has been either manually digitized over aerial imagery or surveyed in-situ with continuous topo RTK-GNSS.

4.3.2 Stake Measurements

As of 2021 over 15 rural Indigenous communities in the Bristol Bay region utilize stake ranging to monitor erosion. The Stakes for Stakeholders program trains environmental coordinators from each community in data collection (Buzard et al., 2019a). Stake ranging uses a permanent landmark or a stake (wooden or metal) to measure the distance to the eroding feature. Several transects are set up perpendicular to the eroding feature with two to three stakes along each transect. The local data collector visits each site every one to three months and before and after big storms.

Two stake ranging sites were set up in Dillingham 2016 with an additional site added in 2021 (**Figure 31**). Measurements are collected by local environmental coordinators every 1-3 months and before and after large storms. The data collectors measure from the site reference point (typically a wooden stake, or other permanent feature) out to the eroding feature. These datasets provide a high resolution look at the most recent shoreline change (**Figures 32 & 33**). They can help better understand shoreline change in terms of recent climate settings, as opposed to the DSAS, which relies on historical imagery. They can also highlight storm events in great detail. Between the start of monitoring and 2016, the ACGL has received thirteen sets of measurements that are reported here. Time-lapse cameras were also set up at each site to capture images every hour (described below).

DRAFT

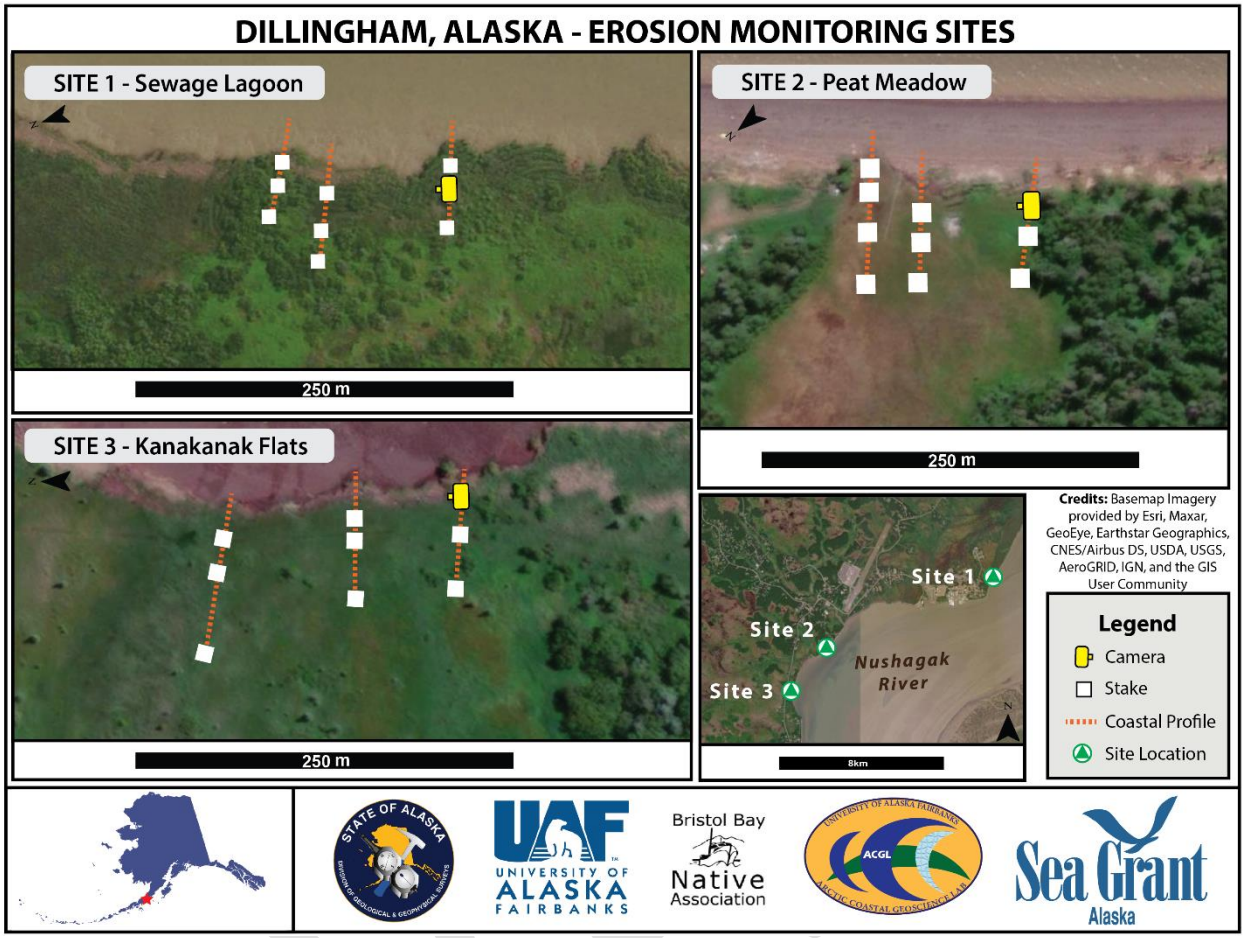


Figure 31. Map of erosion monitoring sites and stake measurement transects. The sites are located on top of a beach ridge fronting the ocean side coastline. Each site consists of a time-lapse camera with 3-4 staked transects where local environmental coordinators take repeat measurements.

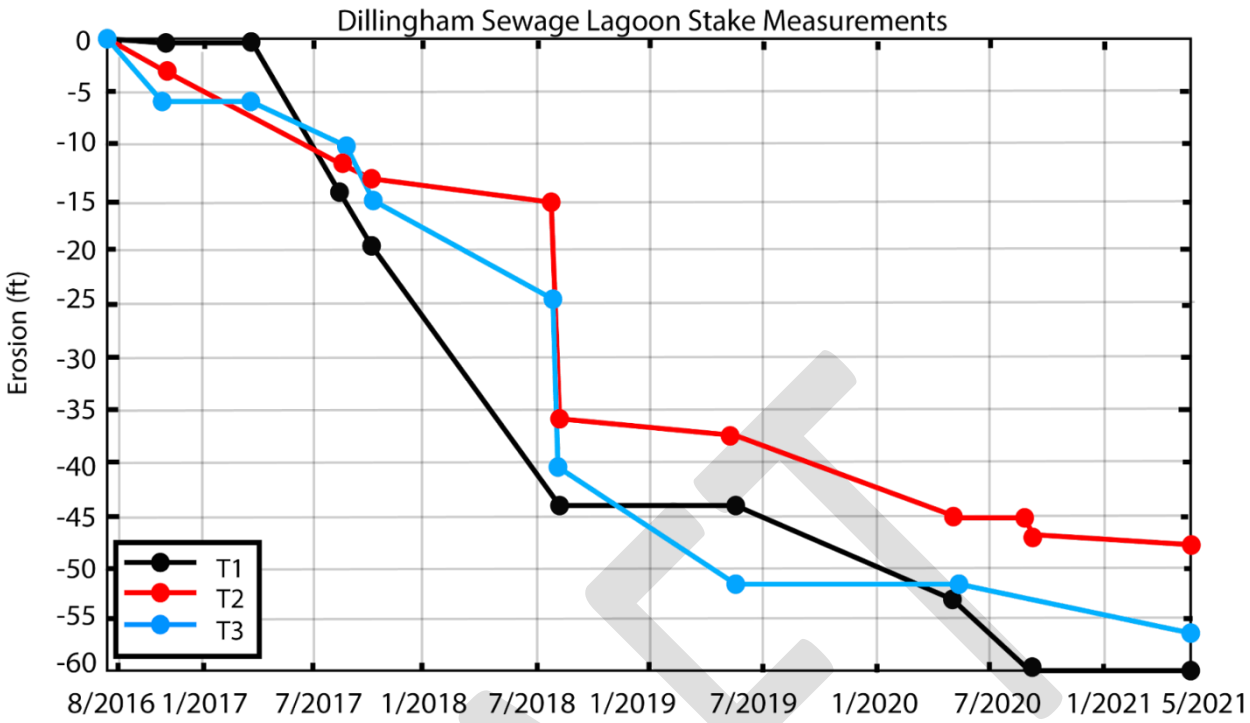


Figure 32. Plotted stake ranging measurements from site 1, sewage lagoon.

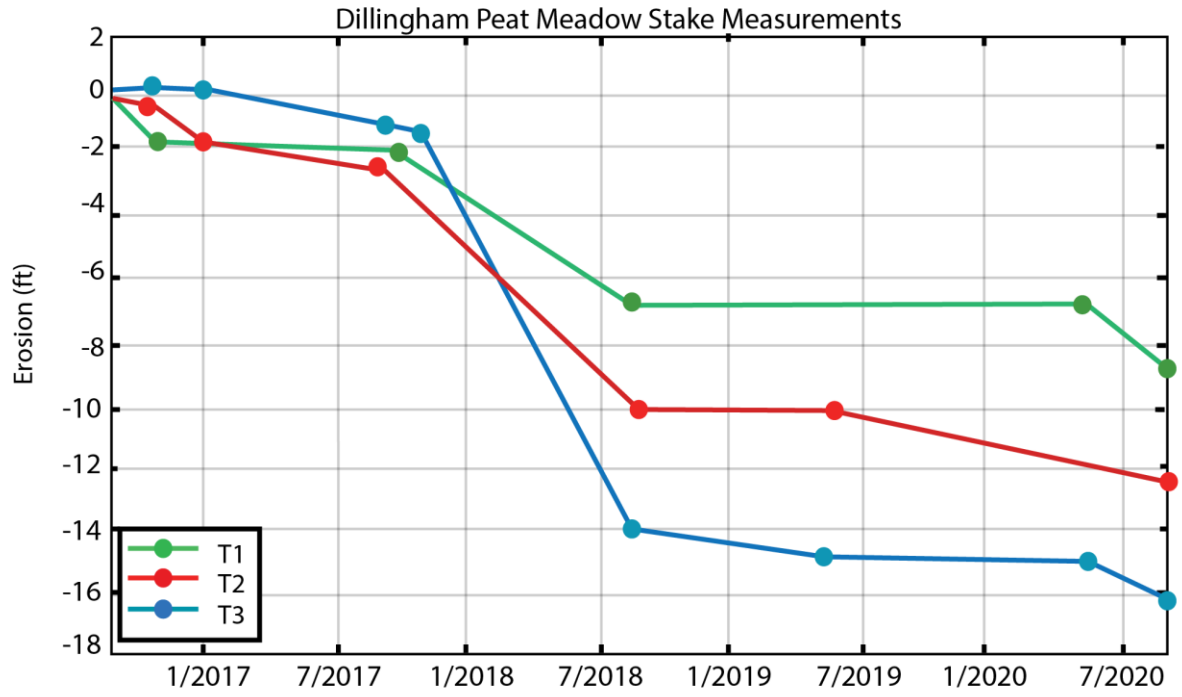


Figure 33. Plotted stake ranging measurements from site 2, peat meadow.

4.3.3 Cross Shore Elevation Profiles

Coastal elevation profiles represent the elevation of the beach from ocean (right) to land (left). When plotted through time, coastal elevation profiles can be used to understand coastal dynamics including the impacts of storms and changing ocean conditions.

Elevation profiles at Dillingham were collected by the ACGL along cross-shore transects at 40+ locations in 2016, 2017, 2018, and 2021, and 2022 (**Figure 34 - 36**).

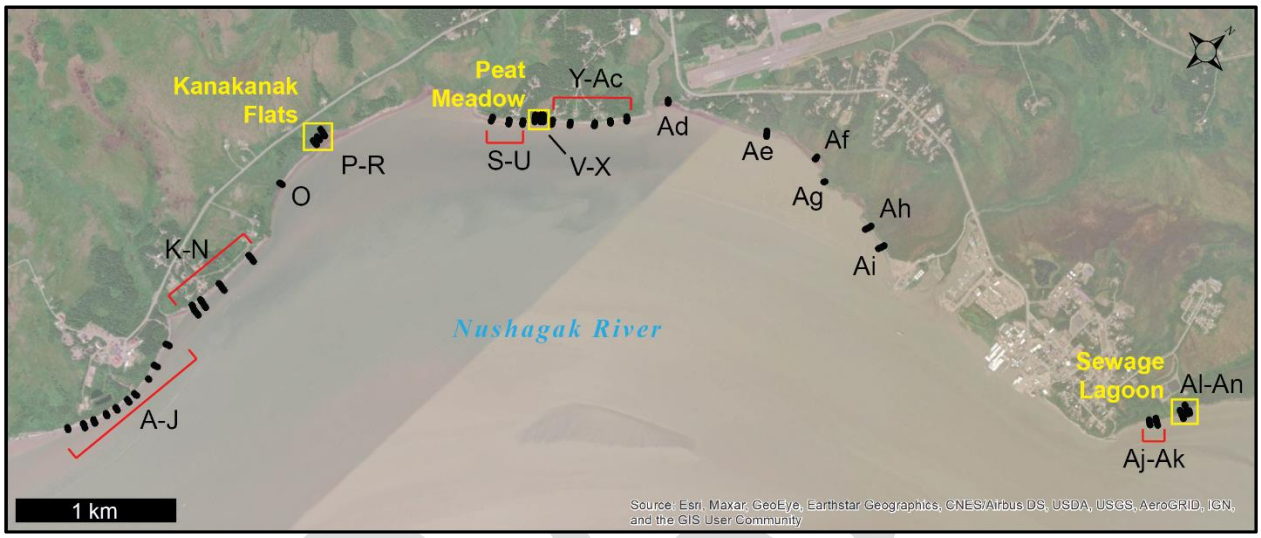


Figure 34. Site map showing the location of cross shore elevation profiles where repeat measurements exist (black labels) as well as erosion monitoring sites (yellow labels).

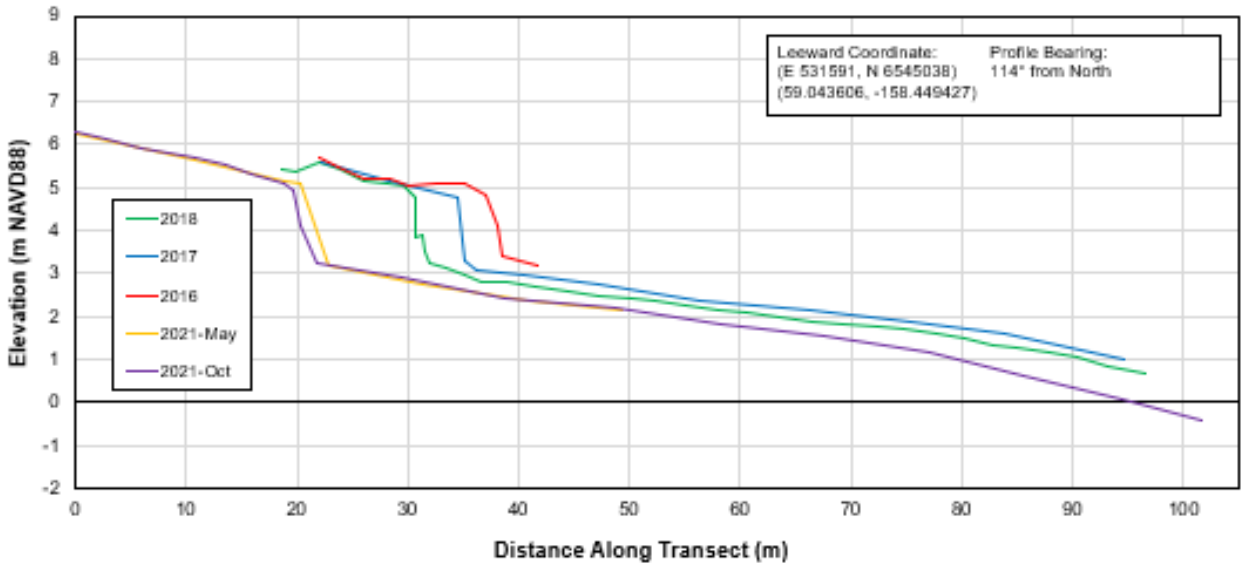


Figure 35. Example cross shore profile from the City Sewage Lagoon with data plotted from 2016, 2017, 2018, May 2021, and Oct 2021. This is profile An (reference figure 34). Notice how much erosion has occurred.

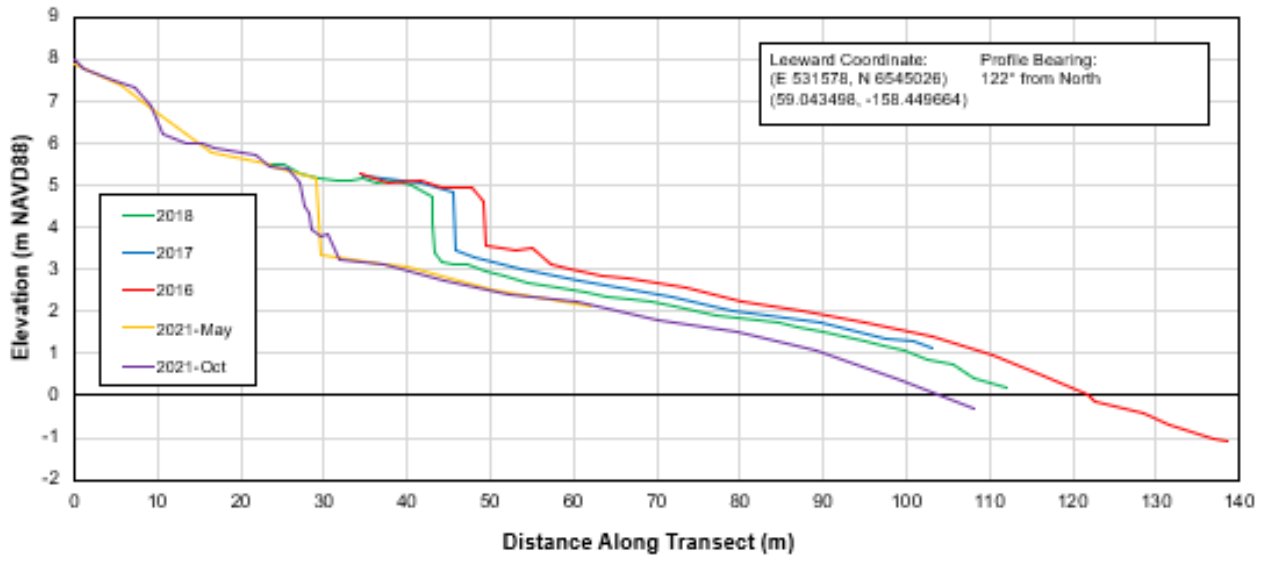


Figure 36. Example cross shore profile from the City Sewage Lagoon with data plotted from 2016, 2017, 2018, May 2021, and Oct 2021. This is profile Ao (reference figure 34). Notice how much erosion has occurred.

4.3.4 Timelapse Photography

As of 2021 over 15 rural Indigenous communities in the Bristol Bay region utilize time lapse imagery for erosion monitoring. The Stakes for Stakeholders program trains environmental coordinators from each community in time-lapse imagery (Buzard et al., 2019a). Cameras are set up perpendicular to a single transect and captures hourly images, then run through a MATLAB code that calculates shoreline change.

Time-lapse cameras were set up at two sites at Dillingham in 2016 and another site was added in 2021. Data is currently being collected. The cameras were oriented perpendicular to a single profile at each site. Images were taken every hour and compiled into time-lapse videos (**Figures 37 & 38**). These datasets visually show change at each shoreline and can capture storm events. They provide a cheap alternative for shoreline change monitoring in remote locations.

DRAFT



Figure 37. Example time-lapse picture of erosion monitoring site 1 located at the Dillingham Sewage Lagoon. Compiled video URL: https://youtu.be/M0zNXxNGhig



Figure 38. Example time-lapse picture of erosion monitoring site 2 located at a peat meadow site in Dillingham. Compiled video URL: https://youtu.be/tnJqI6gD2zw

4.4 HAZARD AND EXPOSURE ASSESSMENTS

Hazard and exposure assessments were generated based on analysis of the baseline datasets and repeat measurements described above. Hazard maps indicate the potential for coastal hazards in a given location, such as flooding or erosion, while exposure maps indicate the proximity of infrastructure or human life to these hazards. For instance, shoreline change analysis describes coastal hazards by quantifying the spatial extent and rates of erosion along the beach, while shoreline change maps indicating areas where critical infrastructure is in close proximity to quickly eroding land constitute an exposure map. These products also require analysis and integration of multiple data sources. Hazard and exposure assessments involve increased interpretation by researchers through the integration of multiple data products into theoretical models and the selection of certain areas that researchers deem to be at-risk. The uncertain nature of these analyses and the subjective interpretation of results should be noted when taking results into account for decision-making.

4.4.1 Flood Hazard Map

The UAF ACGL has not produced a flood hazard map for Dillingham.

4.4.2 Infrastructure Exposure Maps

Developing accurate digital maps of community infrastructure that can be integrated within GIS assessment is an important step in assessing risks. This includes both the horizontal position in relation to the coastline and its elevation above MHW, which allow for an assessment of both erosion and flooding. Infrastructure data layers from the Alaska Division of Community and Regional Affairs (DCRA) were compiled from AutoCAD files and subsequently projected in the State Plane NAD 1983 projection system. Specific infrastructure features were extracted and saved as individual point, line, or polygon features within an ESRI geodatabase, and measurements of feature height were saved, where available (AK DGGS, Personal Communication). Infrastructure features that could be affected by erosion were prioritized, such as buildings, roads, pipes, electric lines, and solid waste disposal locations. Information about the type and purpose of each structure in Dillingham is included and allows for a practical assessment of coastal hazards and their immediate risk to community resources (**Figure 39**).

Infrastructure vulnerable to erosion was identified and categorized by extrapolating the most recent shoreline across a given shoreline section at 10-year intervals using the average WLR rate of that section. There is an assumption of linearity made in this type of analysis which introduces inherent uncertainties due to the non-linearity of many environmental processes.

DRAFT

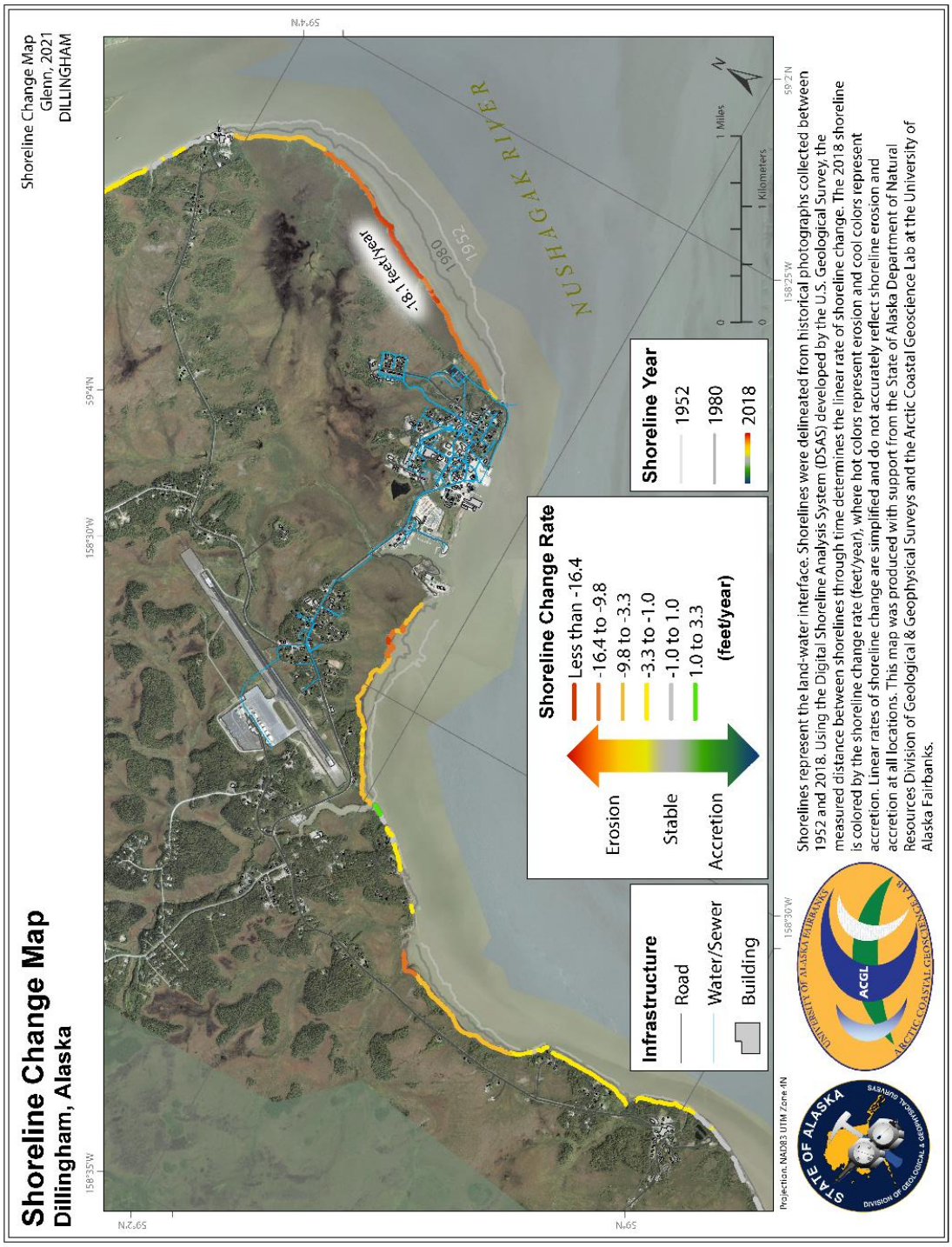


Figure 39. Shoreline change map of the Dillingham area. Warmer colors (red) equate to higher rates of erosion, cooler colors (green-blue) equate to areas with accretion. Shorelines from 1952 and 1980 are included. Roads, water/sewer lines, and buildings are overlaid on the map.

4.4.3 Shoreline Change Analysis

The following subsections display and describe results from the community erosion vulnerability assessment. Results are coupled with infrastructure data layers to quantify the overall risk to the community's buildings and utilities, and project future risks with an assumption of linearity in shoreline change rates. A subsample of the plotted cross-shore elevation profiles from representative sections of the shoreline are presented and discussed.

Important Note: Projected shoreline positions have significant uncertainties brought about by the stochastic non-linear nature of coastal and environmental changes. Future shoreline positions have been determined by extrapolating rates of change based off past movements of the shoreline indicator. As such, projections do not account for accelerated change.

To quantify decadal shoreline change, the lateral position of shorelines around Dillingham was delineated using orthorectified aerial imagery spanning approximately 70 years (Error! Reference source not found.). Net shoreline changes and weighted l inear change rates were calculated using the USGS Digital Shoreline Analysis System (DSAS) by casting cross-shore virtual transects at set intervals from a reference line. The vegetation line (vegline) was selected as the shoreline indicator because it is easily discernable on the ground and in aerial imagery (**Figure 40**), and there is no inherent error due to tidal fluctuations and/or swash action as is the case with other potential indicators.

The average *rate* of change of the area over the 70-year study period was quantified using the weighted linear regression rate-of-change statistic (WLR) computed at each transect along the shoreline. The WLR is supported with a 95% confidence interval (WCI) and R-squared value (WR^2). *Total* change was calculated using the net shoreline movement (NSM) statistic, which describes the distance between the oldest and most recent shoreline along each transect over the study period (Himmelstoss et al., 2018).

Table 7. Summary of aerial and satellite imagery used for shoreline delineation.

Date	Type	Source	Resolution [m^2]	Provider
1952	Aerial	NASA AHAP	4.5	USGS
1982	Aerial	High Altitude	1.0	USGS
2001	Satellite	IKONOS	3.2 (Panc: 0.82)	PGC
2006	Satellite	QUICKBIRD	2.5 (Panc: 0.68)	PGC
2011	Satellite	WorldView I	0.54	PGC
2016	Aerial	Medium Altitude	0.35	NGS/NOAA
2020	Satellite	WorldView II	1.88 (Panc: 0.57)	PGC

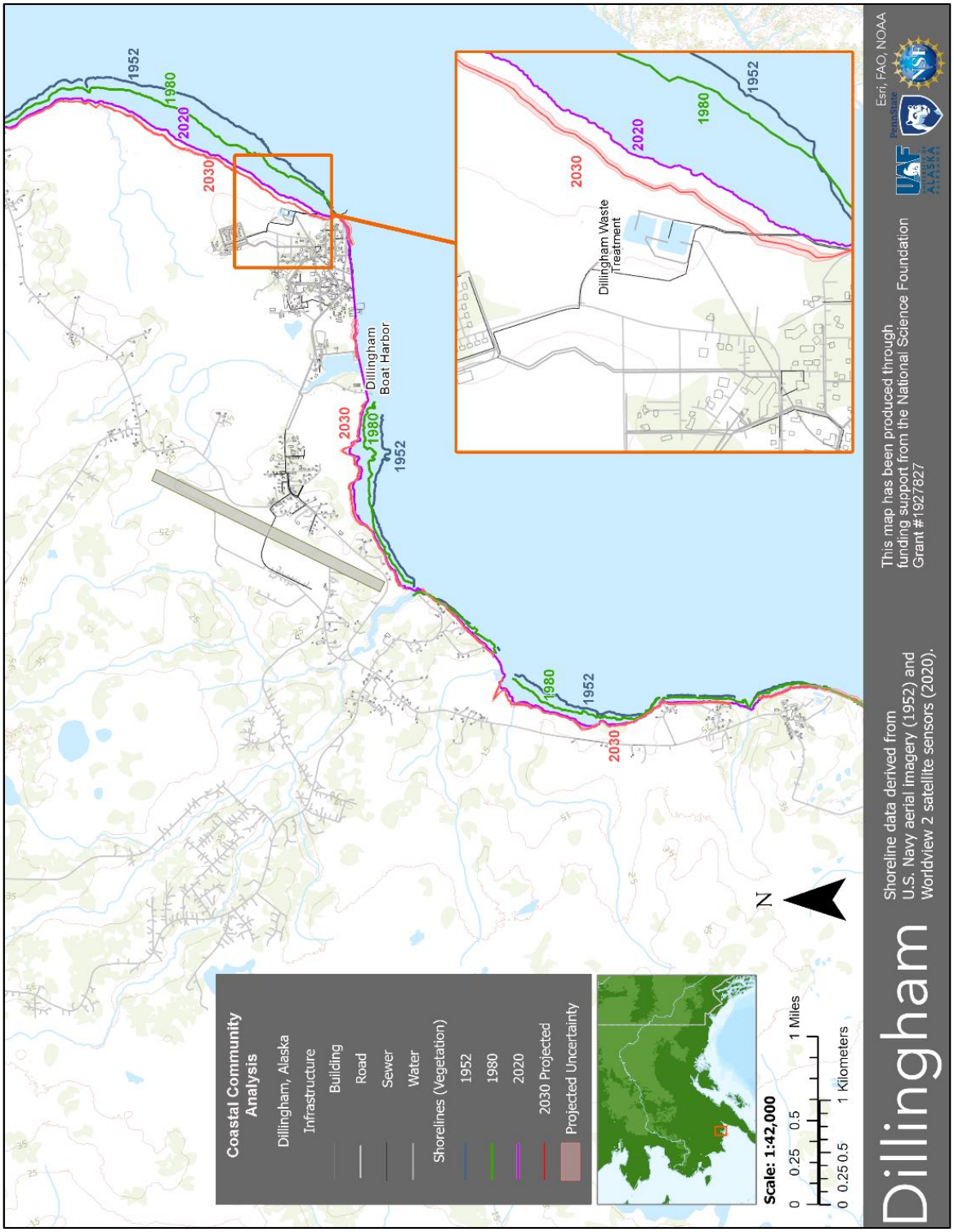


Figure 40. Shoreline change and erosion projection map of the Dillingham area. Shorelines from 1952, 1980, 2020, and 2030 (projected) are provided. Roads, water/sewer lines, and buildings are overlaid on the map.

5. IDENTIFIED COASTAL HAZARD AREAS

This section documents the results of the erosion vulnerability assessment (**Figures 42 & 43**), with an emphasis placed on identifying infrastructure at risk of erosion over spatiotemporal scales relevant to community planning; long term morphodynamic evolution is beyond the scope of this report. Identified coastal hazard areas are identified as such based off erosion rates coupled with proximity to infrastructure or otherwise cultural significant features.

Identified coastal hazard areas in Dillingham are as follows:

1. City Sewage Lagoon
   The city sewage lagoon observed the highest rates of erosion (>5 meters per year) compared to other sites (**Figure 41**). At this location that much can sometimes be lost through a single storm, as was the case in August 2018. The city sewage lagoon is only 120 m away from the actively eroding coastline and has seen almost 200 m of land lost over the last 40 years. Mitigation planning is currently underway.

2. Kanakanak Hospital Sewage Lagoon and Campus
   Erosion just up from the river's mouth has brought the bluff edge to about 35 m from the sewage lagoon of Kanakanak Hospital, which serves the wider Bristol Bay region. Approximately 2 meters of land falls away annually, with approximately 60 m worth of land loss over the last 40 years.
   This site also has bodies of victims from the 1918 influenza pandemic emerging from a mass grave as the ground gives way to the storms.

3. City Harbor and lowlands to the west (Kanakanak Road)
   In addition to erosion of the banks within the City Harbor, the coastline on either side of the harbor is observing significant rates of erosion as well. The main road to the hospital, Kanakanak Road, is within decadal erosion forecasts. Up to 240 m worth of land has eroded away in the last 40 years just west of the City Harbor. The interior of harbor was not included in ACGL's erosion study since the banks are heavily modified due to existing bulkheads and ongoing erosion mitigation projects.

DRAFT

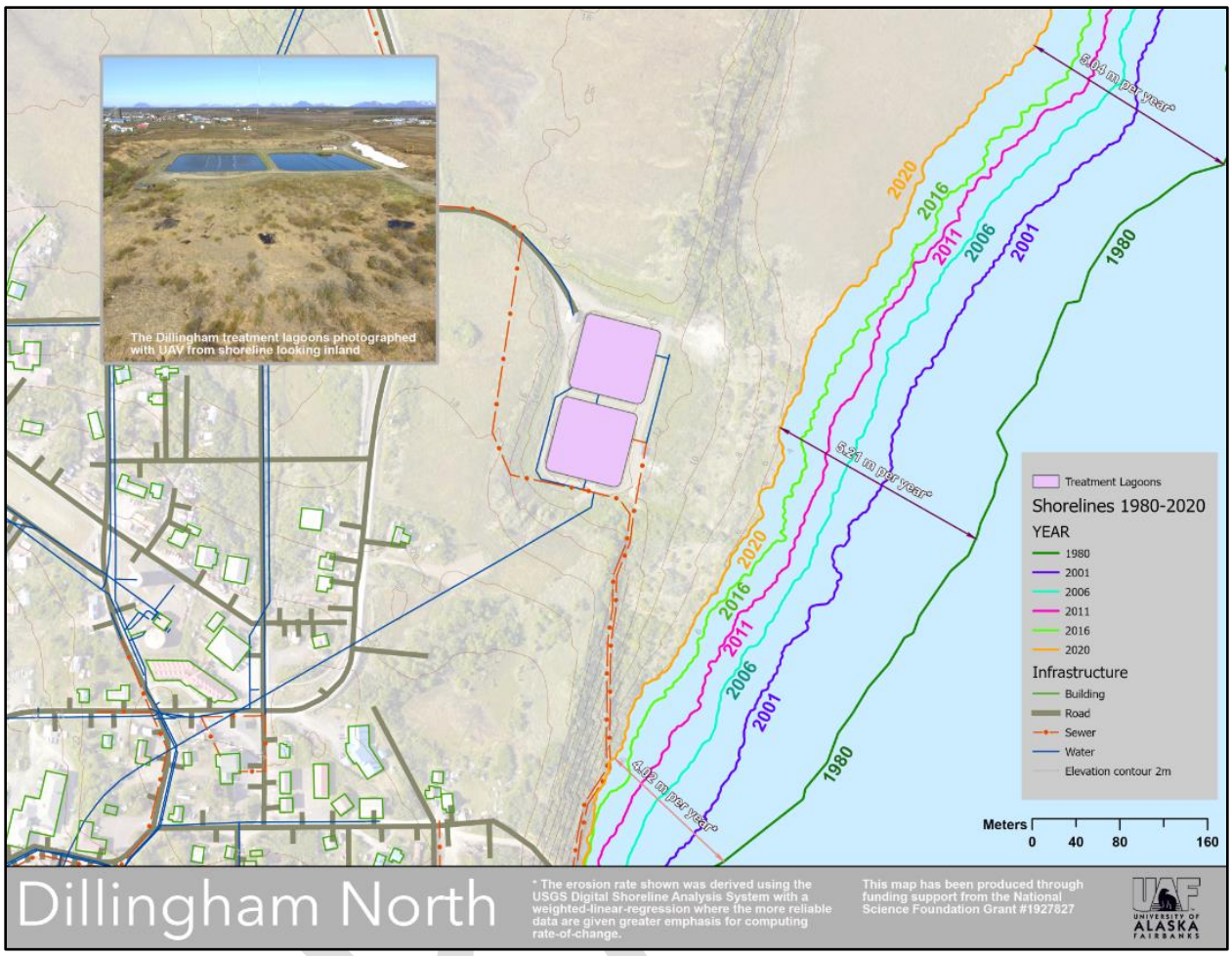


Figure 41. Shoreline change map of the city sewage lagoon. Past shoreline positions are provided along with values of land loss. Notice how much erosion has occurred. Buildings, roads, water/sewer lines, as well as elevation contours are overlaid.

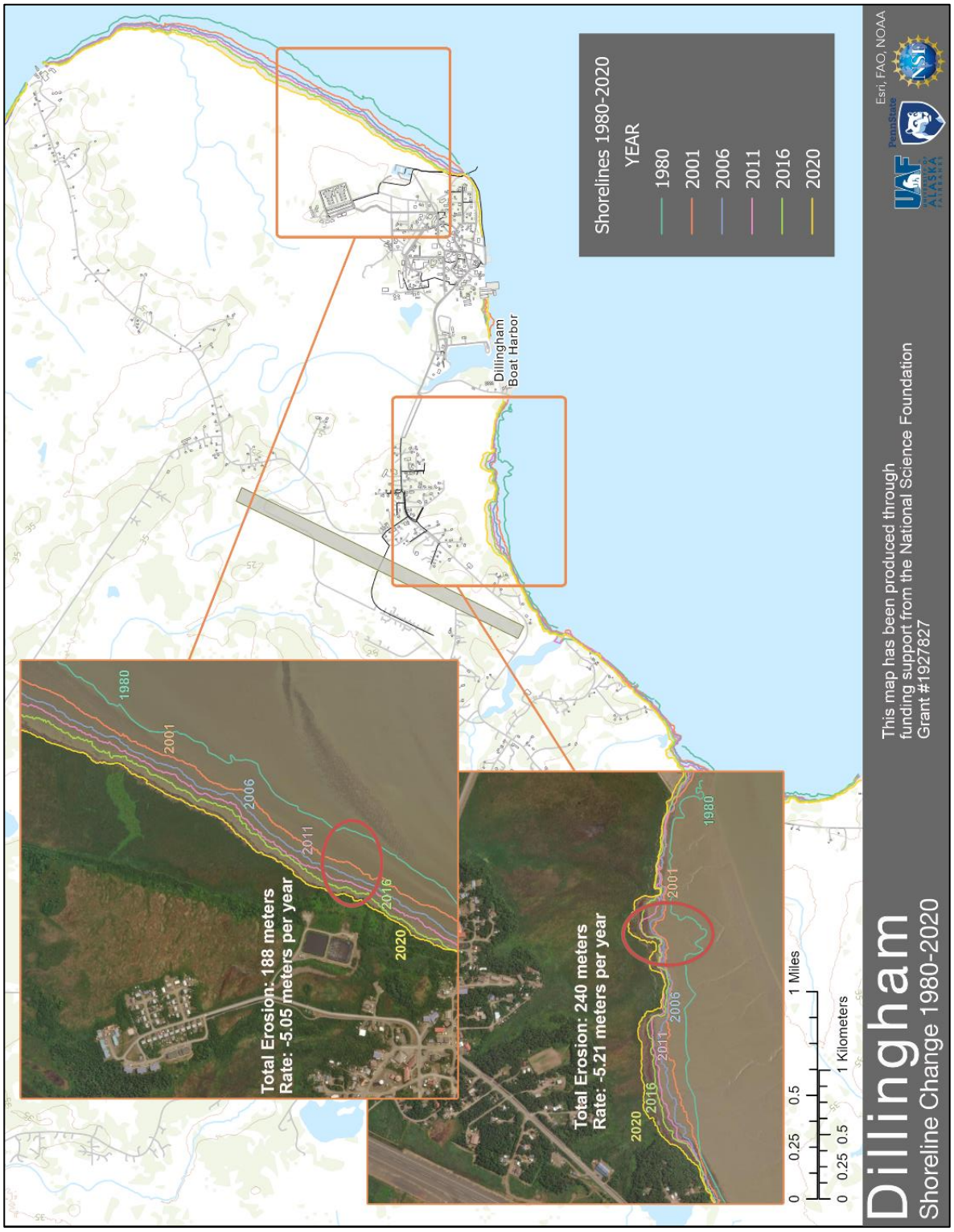


Figure 42. Shoreline change map of the Dillingham area. This map displays the digitized shorelines used in the shoreline change assessment. Roads, water/sewer lines, and buildings are overlaid on the map.

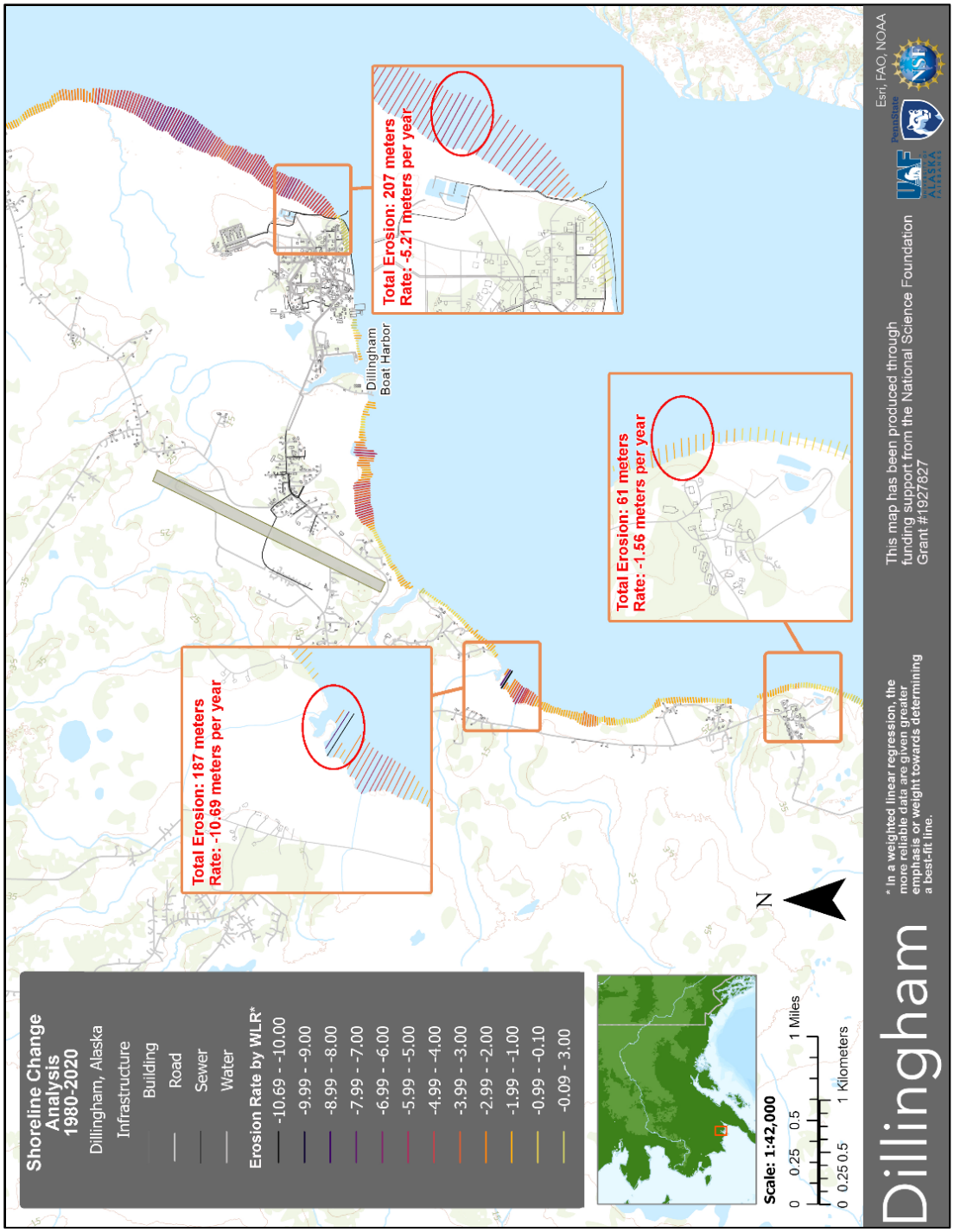


Figure 43. Shoreline change map of the Dillingham area. This map displays clipped shoreline change envelope from the shoreline change analysis. The length of the lines represents how much erosion has occurred over the last 40 years and the color of the lines represent the rate of erosion at that location over the last 40 years. Roads, water/sewer lines, and buildings are overlaid on the map.

6. SUMMARY OF COMMUNITY THREATS AND RESILIENCY

6.1. SUMMARY OF THREATS

- Erosion at Snag Point is the most significant in the study area and is directly threatening the city's sewage lagoon.
- Erosion at the Kanakanak Hospital directly threatens the campus sewage lagoons, burial sites, and archaeology.
- Erosion in and around the city's harbor has been an ongoing issue, but there have been multiple erosion mitigation projects undertaken to address this.

7. DATA GAPS AND FUTURE WORK

7.1. PRIORITY DATA GAPS

While the data products in this report describe coastal processes through their impacts on shorelines and beach profiles, a more thorough understanding of the local oceanographic setting would improve predictions regarding erosion at Dillingham. Additionally, improving understanding of potential storm and flooding impacts is a major goal for mitigation efforts in Dillingham. In order to more accurately assess these risks, additional data products are necessary, including past storm total water levels and building first floor heights (**Table 8**).

Table 8. Summary of data gaps at Dillingham. Applications and expected acquisitions for each item is provided.

Item	Application(s)	Exp. Acquisition
Past Storm TWLs	Developing a historical index of past storm events; informing city planning and decision making	TBD
First Floor Heights	Accurately assess flooding vulnerability, informing city planning and decision making	TBD
Real Time Ocean Monitoring	Accurately assess erosion and flooding vulnerability, informing city planning and decision making	Summer 2021 – Continuous

7.2. ACGL FUTURE WORK

Continued work is being carried out to improve the vulnerability assessment of Dillingham and another field work campaign is planned for Summer 2022. This will include deployment of a wave buoy, repeat beach profiles and UAV surveys, along with continued correspondence with members of the community. These datasets will feed into the comprehensive coastal hazard assessment produced by ACGL and will be updated annually.

DRAFT

8. CITATIONS

Citations of reports and assessments directly pertaining to Dillingham are bolded.

ADEC, Alaska Department of Environmental Conservation, 2004. Source water assessment, A hydrogeologic susceptibility and vulnerability assessment for Nelson Lagoon water system. Report PWSID#260804.001.

ADLWD, Alaska Department of Labor and Workforce Development., 2011. Alaska Local and Regional Information: Nelson Lagoon.

Agisoft, L.L.C. and St Petersburg, R., 2019. Agisoft Metashape User Manual: Professional Edition.

Agisoft, L.L.C. and St Petersburg, R., 2019. Agisoft Metashape User Manual: Professional Edition.

Alaska Department of Community and Regional Affairs, 1982, Dillingham, community profile: Prepared by DOWL Engineers for the Alaska Department of Community and Regional Affairs, 2 sheets.

Alaska State Housing Authority, 1971, Dillingham reconnaissance report and initial housing element, April, 1970: Anchorage, p. 11-22.

Antunes, N.S.M., 2000. The Importance of the tidal datum in the definition of maritime limits and boundaries. Ibru.

AOOS, Alaska Ocean Observing System, 2014. Data from: Historical Sea Ice Atlas: Alaska Sea Ice, Mid-1800s to the Present. Fairbanks: University of Alaska.

ASOS, Automated Surface Observing System Users Guide, 1998. National Weather Service ASOS Program Office, 74 pp.

Atkinson, D.E., 2005. Observed storminess patterns and trends in the circum-Arctic coastal regime. Geo-Marine Letters, 25(2-3), pp.98-109.

Bader, J., Mesquita, M.D., Hodges, K.I., Keenlyside, N., Østerhus, S. and Miles, M., 2011. A review on Northern Hemisphere sea-ice, storminess and the North Atlantic Oscillation: Observations and projected changes. Atmospheric Research, 101(4), pp.809-834.

Barnhart, K.R., Overeem, I. and Anderson, R.S., 2014. The effect of changing sea-ice on the physical vulnerability of Arctic coasts. The Cryosphere, 8(5), pp.1777-1799.

Beikman, H.M., 1974, Preliminary geologic map of the southwest quadrant of Alaska: U.S. Geological Survey Miscellaneous Field Investigations Map MF-611, 2 sheets, scale 1:100,000.

Bogardus, R., Maio, C., Mason, O., Buzard, R., Mahoney, A. and de Wit, C., 2020. Mid-Winter Breakout of Landfast Sea Ice and Major Storm Leads to Significant Ice Push Event Along Chukchi Sea Coastline. Frontiers in Earth Science, 8, p.344.

Brower Jr, W.A., Diaz, H.F., Prechtel, A.S., Searby, H.W. and Wise, J.L., 1977. Climatic Atlas of the Outer Continental Shelf Waters and Coastal Regions of Alaska. Volume II. Bering Sea. alaska univ anchorage arctic environmental information and data center.

Brower, W.A., Jr., Diaz, H.F., Prechtel, A.S., Searby, H.W., and Wise, J.L., 1977, Climatic atlas of the outer continental shelf waters and coastal regions of Alaska: U.S. Department of Commerce, National Oceanic and Atmospheric

Administration, Alaska Outer Continental Shelf Environmental Assessment Program Final Report Research Unit 347, 443 p.
Buzard, R., Maio, C.V., Kinsman, N., and Verbyla, D., 2020. Shoreline change analysis of Goodnews Bay, Alaska. Shore and Beach, 88(2), pp. 1-13.
Buzard, R.M., 2017. Spatiotemporal patterns of bluff erosion at Goodnews Bay, Alaska. University of Alaska Fairbanks. Master's thesis.
Buzard, R.M., Overbeck, J.R., and Maio, C.V., 2019a, Community-based methods for monitoring coastal erosion: Alaska Division of Geological & Geophysical Surveys Information Circular 84, 35 p. http://doi.org/10.14509/30182
Buzard, R.M., Overbeck, J.R., and Maio, C.V., 2019b. Baseline shoreline assessment using time-lapse photography and emery rods. Environmental Protection Agency Quality Assurance Project Plan. Approved 3/8/2017, updated and approved 4/11/2019.
Cacchione, D.A. and Drake, D.E., 1979. A new instrument system to investigate sediment dynamics on continental shelves. Marine Geology, 30(3-4), pp.299-312.
Cazenave, A., Meyssignac, B., Ablain, M., Balmaseda, M., Bamber, J., Barletta, V., Beckley, B., Benveniste, J., Berthier, E., Blazquez, A. and Boyer, T., 2018. Global sea-level budget 1993-present. Earth System Science Data, 10(3), pp.1551-1590.
CE2 Engineers, Inc., 2002. Water system improvement plan, Nelson Lagoon, Alaska. Prepared for Nelson Lagoon Council.
Cooper, A.K., Marlow, M.S. and Scholl, D.W., 1976. Mesozoic magnetic lineations in the Bering Sea marginal basin. Journal of Geophysical Research, 81(11), pp.1916-1934.
Davidson-Arnott, R., Bauer, B. and Houser, C., 2019. Introduction to coastal processes and geomorphology. Cambridge university press.
Davies, J., Sykes, L., House, L. and Jacob, K., 1981. Shumagin seismic gap, Alaska Peninsula: History of great earthquakes, tectonic setting, and evidence for high seismic potential. Journal of Geophysical Research: Solid Earth, 86(B5), pp.3821-3855.
Dean, B., Collins, I., Divoky, D., Hatheway, D. and Scheffner, C.N., 2005. FEMA Coastal Flood Hazard Analysis and Mapping Guidelines Focused Study Report.
Dillingham Hazard Mitigation Plan (HMP), 2016, Prepared by The City of Dillingham Hazard Mitigation Planning Team, p. 244.
Donnelly, C., Kraus, N. and Larson, M., 2006. State of knowledge on measurement and modeling of coastal overwash. Journal of coastal research, 22(4 (224)), pp.965-991.
Dygas, J.A. and Burrell, D.C., 1976. Wind and current patterns in an arctic coast Lagoon. Ocean Engineering, 3(5), pp.317-327.
Emery, K.O., 1961. A simple method of measuring beach profiles. Limnology and Oceanography, 6(1), pp.90-93.
Environmental Protection Agency (EPA), 2021. About Bristol Bay. Available at: https://www.epa.gov/bristolbay/about-bristol-bay (accessed: January 14, 2022).
Erikson, L.H., Espejo, A., Barnard, P.L., Serafin, K.A., Hegermiller, C.A., O'Neill, A., Ruggiero, P., Limber, P.W. and Mendez, F.J., 2018. Identification of storm events

and contiguous coastal sections for deterministic modeling of extreme coastal flood events in response to climate change. Coastal Engineering, 140, pp.316-330.

Farquharson, L.M., Mann, D.H., Swanson, D.K., Jones, B.M., Buzard, R.M. and Jordan, J.W., 2018. Temporal and spatial variability in coastline response to declining sea-ice in northwest Alaska. Marine Geology, 404, pp.71-83.

Federal Emergency Management Agency (FEMA), 1982, Flood insurance study, city of Dillingham, Alaska, Bristol Bay division: 16 p.

Fok, H.S., 2012. Ocean tides modeling using satellite altimetry (Doctoral dissertation, The Ohio State University).

Forbes, D.L., 2011. State of the Arctic coast 2010: scientific review and outlook. Land-Ocean Interactions in the Coastal Zone, Institute of Coastal Research.

Francis, J.A., Chen, Y., Miller, J.R. and Russell, G., 2011, December. Projected regime shift in arctic feedbacks. In AGU Fall Meeting Abstracts (Vol. 2011, pp. A31D-0107).

Frey, K.E., Moore, G.W.K., Cooper, L.W. and Grebmeier, J.M., 2015. Divergent patterns of recent sea-ice cover across the Bering, Chukchi, and Beaufort seas of the Pacific Arctic Region. Progress in Oceanography, 136, pp.32-49.

Freymueller, J.T., 2013. Vertical Analytical Model for Vertical Crustal Deformation in Alaska.

Fu, L.L. and Pihos, G., 1994. Determining the response of sea level to atmospheric pressure forcing using TOPEX/POSEIDON data. Journal of Geophysical Research: Oceans, 99(C12), pp.24633-24642.

Gindraux, S., Boesch, R. and Farinotti, D., 2017. Accuracy assessment of digital surface models from unmanned aerial vehicles' imagery on glaciers. Remote Sensing, 9(2), p.186.

Glaeser, J.D., 1978. Global distribution of barrier islands in terms of tectonic setting. The Journal of Geology, 86(3), pp.283-297.

Glass, R.L., 1987, Water resources near Dillingham in the Bristol Bay area, Alaska: U.S. Geological Survey Water-Resources Investigations Report 87-4141, 27 p.

Golder Associates Inc., 2007. Ekuk Village erosion assessment. Prepared for Ekuk Village Council by Rowland Atkins. Anchorage, AK, 48 pp., ref: 073-95052.

Goodwin, I.D., Ribó, M. and Mortlock, T., 2020. Coastal sediment compartments, wave climate and centennial-scale sediment budget. In Sandy Beach Morphodynamics (pp. 615-640). Elsevier.

Gornitz, V., 1995. Sea-level rise: A review of recent past and near-future trends. Earth surface processes and landforms, 20(1), pp.7-20.

Grow, J.A. and Atwater, T., 1970. Mid-Tertiary tectonic transition in the Aleutian arc. Geological Society of America Bulletin, 81(12), pp.3715-3722.

Hartman, C.W, and Johnson, PR., 1984, Environmental atlas of Alaska: University of Alaska, Fairbanks, Institute of Water Resources/Engineering Experiment Station, 95 p.

HDR, 2011. Nelson Lagoon Hazard Impact Study, Prepared for the Aleutians East Borough.

HDR, 2014a. Nelson Lagoon Coastal Erosion Study Numerical Hydrodynamic Model Technical Memorandum, Prepared for the Aleutians East Borough.

DRAFT

HDR, 2014b. Nelson Lagoon Coastal Erosion Study Numerical Wave Model Technical Memorandum, Prepared for the Aleutians East Borough.
HDR, 2014c. Nelson Lagoon Coastal Erosion Study Historical Shoreline Map Report, Prepared for the Aleutians East Borough.
HDR, 2015. Nelson Lagoon Shoreline Protection 20% Preliminary Design. Project No. 213165. Prepared for the Aleutians East Borough.
Herring, S.C., Christidis, N., Hoell, A., Kossin, J.P., Schreck III, C.J. and Stott, P.A., 2018. Explaining extreme events of 2016 from a climate perspective. Bulletin of the American Meteorological Society, 99(1), pp. S1-S157.
Himmelstoss, E.A., Henderson, R.E., Kratzmann, M.G. and Farris, A.S., 2018. Digital Shoreline Analysis System (DSAS) version 5.0 user guide (No. 2018-1179). US Geological Survey.
Hoyt, J.H., 1967. Barrier island formation. Geological Society of America Bulletin, 78(9), pp.1125-1136.
Hubertz, J.M., 1992. A users guide to the WIS wave model, Version 2.0, WIS report 27, U.S. Army Engineer Waterways Experiment Station, Vicksburg, MS.
Hume, J.D. and Schalk, M., 1967. Shoreline processes near Barrow, Alaska: a comparison of the normal and the catastrophic. Arctic, pp.86-103
Hunter, R.E., Sallenger, A.H. and Dupré, W.R., 1979. Maps showing directions of longshore sediment transport along the Alaskan Bering Sea Coast (No. 1049).
Iowa State University. 2020 “ASOS-AWOS-Metar Data Download.” Retrieved 10/20/2020 from https://mesonet.agron.iastate.edu/request/download.phtml?network=AK_ASOS
James, M.R., Robson, S. and Smith, M.W., 2017. 3-D uncertainty-based topographic change detection with structure-from-motion photogrammetry: precision maps for ground control and directly georeferenced surveys. Earth Surface Processes and Landforms, 42(12), pp.1769-1788.
Johnson, E.A., 1983. Textural and compositional sediment characteristics of the southeastern Bristol Bay continental shelf, Alaska (Doctoral dissertation, California State University, Northridge).
Jones, S.C., Harr, P.A., Abraham, J., Bosart, L.F., Bowyer, P.J., Evans, J.L., Hanley, D.E., Hanstrum, B.N., Hart, R.E., Lalaurette, F. and Sinclair, M.R., 2003. The extratropical transition of tropical cyclones: Forecast challenges, current understanding, and future directions. Weather and Forecasting, 18(6), pp.1052-1092.
Kinder, T.H. and Schumacher, J.D., 1981. Circulation Over the Continental Shelf. The eastern Bering Sea shelf: oceanography and resources, 1, p.53.
Kinsman, N.E. and DeRaps, M.R., 2012. Coastal hazard field investigations in response to the November 2011 Bering Sea storm, Norton Sound, Alaska. Report of Investigations, p.2.
Kinsman, N.E. and Gould, A., 2014. Contemporary shoreline retreat rates at Meshik in Port Heiden, Alaska. State of Alaska, Department of Natural Resources, Division of Geological & Geophysical Surveys.
Kinsman, N.E., DeRaps, M.R. and Smith, J.R., 2013. Preliminary Evaluation of Coastal Geomorphology and Geohazards on" Kigiqtam Iglua," an Island Northeast of

Shishmaref, Alaska. Alaska: Alaska Department of Natural Resources, Division of Geological & Geophysical Surveys.

Laporte-Fauret, Q., Marieu, V., Castelle, B., Michalet, R., Bujan, S. and Rosebery, D., 2019. Low-cost UAV for high-resolution and large-scale coastal dune change monitoring using photogrammetry. Journal of Marine Science and Engineering, 7(3), p.63.

Mancini, F., Dubbini, M., Gattelli, M., Stecchi, F., Fabbri, S. and Gabbianelli, G., 2013. Using unmanned aerial vehicles (UAV) for high-resolution reconstruction of topography: The structure from motion approach on coastal environments. Remote sensing, 5(12), pp.6880-6898.

Mangor, K., Drønen, N., Kærgaard, K., Kristensen, S.,E., 2017: Shoreline Management Guidline, DHI, Danmark, 2017, DHI ebook, www.dhigroup.com, 466 pp.

Marlow, M.S., Scholl, D.W., Cooper, A.K. and Buffington, E.C., 1976. Structure and evolution of Bering Sea shelf south of St. Lawrence Island. AAPG Bulletin, 60(2), pp.161-183.

Mason, O.K., Salmon, D.K. and Ludwig, S.L., 1996. The periodicity of storm surges in the Bering Sea from 1898 to 1993, based on newspaper accounts. Climatic Change, 34(1), pp.109-123.

Melvin, A.M., Larsen, P., Boehlert, B., Neumann, J.E., Chinowsky, P., Espinet, X., Martinich, J., Baumann, M.S., Rennels, L., Bothner, A. and Nicolsky, D.J., 2017. Climate change damages to Alaska public infrastructure and the economics of proactive adaptation. Proceedings of the National Academy of Sciences, 114(2), pp.E122-E131.

Mesquita, M.S., 2009. Characteristics and variability of storm tracks in the North Pacific, Bering Sea and Alaska (Doctoral dissertation).

Mesquita, M.S., Atkinson, D.E. and Hodges, K.I., 2010. Characteristics and variability of storm tracks in the North Pacific, Bering Sea, and Alaska. Journal of Climate, 23(2), pp.294-311.

Morton, R.A., Ward, G.H. and White, W.A., 2000. Rates of sediment supply and sea-level rise in a large coastal lagoon. Marine Geology, 167(3-4), pp.261-284.

National Oceanic and Atmospheric Administration (NOAA), 2009, Coastal Inundation Mapping Guidebook: Charleston, SC, Coastal Services Center, 26 p.

National Wildlife Federation (NWF), 2021. Bristol Bay. Available at : https://www.nwf.org/Educational-Resources/Wildlife-Guide/Wild-Places/Bristol-Bay (accessed January 14, 2022).

Nelson Lagoon SECD, Strategic economic plan, 2001. Prepared for the Native Village of Nelson Lagoon by Stadium Group, pp. 1-56

NOAA, National Oceanic and Atmospheric Administration, 2020. Data from: Water Levels - NOAA Tides, and Currents. Silver Spring, MD: NOAA.

Overbeck, J., Buzard, R. and Maio, C., 2017, September. Storm impacts in western alaska documenting shoreline change and flooding through remote sensing and communitybased monitoring. In Oceans 2017-Anchorage (pp. 1-6). IEEE.

Overbeck, J., Buzard, R. and Maio, C., 2019. Community-based methods for monitoring coastal erosion: a step-by-step guide for documenting shoreline change in your community.

Overbeck, J.R., Buzard, R.M., Turner, M.M., Miller, K.Y., and Glenn, R.J., 2020, Shoreline change at Alaska coastal communities: Alaska Division of Geological & Geophysical Surveys Report of Investigation 2020-10, 29 p., 47 sheets.

Overbeck, J.R., ed., 2018, Alaska coastal mapping gaps & priorities: Alaska Division of Geological & Geophysical Surveys Information Circular 72, 34 p.

Overeem, I., Anderson, R.S., Wobus, C.W., Clow, G.D., Urban, F.E. and Matell, N., 2011. Sea-ice loss enhances wave action at the Arctic coast. Geophysical Research Letters, 38(17).

Overland, J.E. and Pease, C.H., 1982. Cyclone climatology of the Bering Sea and its relation to sea-ice extent. Monthly Weather Review, 110(1), pp.5-13.

Palcsak, B.B. and Dorava, J.M., 1994. *Overview of environmental and hydrogeologic conditions at Dillingham, Alaska*. US Department of the Interior, US Geological Survey.

Rachold, V., Are, F.E., Atkinson, D.E., Cherkashov, G. and Solomon, S.M., 2005. Arctic coastal dynamics (ACD): An introduction. Geo-Marine Letters, 25(2-3), pp.63-68.

Reimnitz, E., Dethleff, D. and Nürnberg, D., 1994. Contrasts in Arctic shelf sea-ice regimes and some implications: Beaufort Sea versus Laptev Sea. Marine Geology, 119(3-4), pp.215-225.

Rieger, Samuel, 1965, Soils of the Dillingham area, Alaska: U.S. Soil Conservation Service report, 18 p.

Rieger, Samuel, Schoephorster, D.B., and Furbush, C.E., 1979, Exploratory soil survey of Alaska: U.S. Soil Conservation Service, 213 p.

Rodionov, S.N., Bond, N.A. and Overland, J.E., 2007. The Aleutian Low, storm tracks, and winter climate variability in the Bering Sea. Deep Sea Research Part II: Topical Studies in Oceanography, 54(23-26), pp.2560-2577.

Ruggiero, P., Holman, R.A. and Beach, R.A., 2004. Wave run-up on a high-energy dissipative beach. Journal of Geophysical Research: Oceans, 109(C6). 90

Ruggiero, P., Komar, P.D., McDougal, W.G., Marra, J.J. and Beach, R.A., 2001. Wave run-up, extreme water levels and the erosion of properties backing beaches. Journal of coastal research, pp.407-419.

Sallenger Jr, A.H., 2000. Storm impact scale for barrier islands. Journal of Coastal Research, pp.890-895.

Sallenger Jr, A.H., Howard, P.C., Fletcher III, C.H. and Howd, P.A., 1983. A system for measuring bottom profile, waves and currents in the high-energy nearshore environment. Marine Geology, 51(1-2), pp.63-76.

Sepp, M. and Jaagus, J., 2011. Changes in the activity and tracks of Arctic cyclones. Climatic Change, 105(3), pp.577-595.

Smith, N. and Sattineni, A., 2016. Effect of erosion in Alaskan coastal villages. 52nd Associated Schools of Construction, Provo, Utah.

Sorteberg, A. and Walsh, J.E., 2008. Seasonal cyclone variability at 70 N and its impact on moisture transport into the Arctic. Tellus A: Dynamic Meteorology and Oceanography, 60(3), pp.570-586.

Spargo, E., Hess, K., Myers, E., Yang, Z. and Wong, A., 2006. Tidal datum modeling in support of NOAA's vertical datum transformation tool. In Estuarine and Coastal Modeling (2005) (pp. 523-536).

DRAFT

Stabeno, P.J., Farley Jr, E.V., Kachel, N.B., Moore, S., Mordy, C.W., Napp, J.M., Overland, J.E., Pinchuk, A.I. and Sigler, M.F., 2012. A comparison of the physics of the northern and southern shelves of the eastern Bering Sea and some implications for the ecosystem. Deep Sea Research Part II: Topical Studies in Oceanography, 65, pp.14-30.

Suleimani, E.N., Nicolsky, D.J., and Salisbury, J.B., 2020, Regional tsunami hazard assessment for communities of Bristol Bay and the Pribilof Islands, Alaska: Alaska Division of Geological & Geophysical Surveys Report of Investigation 2020-1, 32 p., 6 sheets.

Thoman, R.L., Bhatt, U.S., Bieniek, P.A., Brettschneider, B.R., Brubaker, M., Danielson, S., Labe, Z., Lader, R., Meier, W.N., Sheffield, G. and Walsh, J.E., 2020. The record low Bering sea-ice extent in 2018: context, impacts, and an assessment of the role of anthropogenic climate change.

Thomson, J. and Rogers, W.E., 2014. Swell and sea in the emerging Arctic Ocean. Geophysical Research Letters, 41(9), pp.3136-3140.

Thomson, J., Fan, Y., Stammerjohn, S., Stopa, J., Rogers, W.E., Girard-Ardhuin, F., Ardhuin, F., Shen, H., Perrie, W., Shen, H. and Ackley, S., 2016. Emerging trends in the sea state of the Beaufort and Chukchi seas. Ocean Modelling, 105, pp.1-12.

Tiernan, A., T. Elison, T. Sands, J. Head, S. Vega, and G. Neufeld. 2021. 2020 Bristol Bay annual management report. Alaska Department of Fish and Game, Fishery Management Report No. 21-16, Anchorage.

Tryck, Nyman and Hayes, 1985, City of Dillingham comprehensive plan, 1985: Anchorage, p. 29-52.

Tschetter, T., Kinsman, N.E. and Fish, A., 2014. Color-indexed elevation maps for flood-vulnerable coastal communities in western Alaska. State of Alaska, Department of Natural Resources, Division of Geological & Geophysical Surveys.

USACE, United States Army Corps of Engineers., 2007. Alaska baseline erosion assessment, erosion information paper – Nelson Lagoon, Alaska.

USACE, United States Army Corps of Engineers., 2009. Alaska Baseline Erosion Assessment Erosion Information Paper – Egegik, Alaska.

USACE, United States Army Corps of Engineers., 2009. Engineering Documentation Report Environmental Assessment and Finding of No Significant Impact - City Shoreline Emergency Bank Stabilization, Dillingham, Alaska.

Vaught, Douglas. 2016. “Nelson Lagoon, Alaska Wind and Solar Resource Assessment Report.” *V3 Energy LLC.* https://www.v3energy.com/wp-content/uploads/2017/04/Nelson-Lagoon-Wind-and-Solar-Resource-Assessment-Report.pdf

Vessey, A.F., Hodges, K.I., Shaffrey, L.C. and Day, J.J., 2020. An inter-comparison of Arctic synoptic scale storms between four global reanalysis datasets. Climate Dynamics, 54(5), pp.2777-2795.

Wahrhaftig, C., 1965. Physiographic divisions of Alaska.

Watanabe, Y. and Kawahara, Y., 2016. UAV photogrammetry for monitoring changes in river topography and vegetation. Procedia Engineering, 154, pp.317-325.

WEAR, Waste Erosion Assessment and Review., 2015. Detailed action plan Nelson Lagoon landfill, 6 p.

Weaver, R.J., 2008. Storm surge: influence of bathymetric fluctuations and barrier islands on coastal water levels. University of Florida.

Wesson, R.L., Boyd, O.S., Mueller, C.S., Bufe, C.G., Frankel, A.D. and Petersen, M.D., 2007. Revision of time-independent probabilistic seismic hazard maps for Alaska. US Geological Survey Open-File Report, 1043(2007), p.33.

Wilson, F.H., Hults, C.P., Mull, C.G, and Karl, S.M, comps., 2015, Geologic map of Alaska: U.S. Geological Survey Scientific Investigations Map 3340, pamphlet 196 p., 2 sheets, scale 1:1,584,000, http://dx.doi.org/10.3133/sim3340.

Wise, J.L., Leslie, L.D. and Labelle, J.C., 1987. *An Oceanographic and Climatological Atlas of Bristol Bay*. ALASKA UNIV ANCHORAGE ARCTIC ENVIRONMENTAL INFORMATION AND DATA CENTER.

WMO, World Meteorological Organization. Commission for Maritime Meteorology, 1970. The Beaufort Scale of Wind Force: (technical and operational Aspects) (No. 3).

Wuebbles, D.J., Fahey, D.W., Hibbard, K.A., Arnold, J.R., DeAngelo, B., Doherty, S., Easterling, D.R., Edmonds, J., Edmonds, T., Hall, T. and Hayhoe, K., 2017. Climate science special report: Fourth national climate assessment (NCA4), Volume I.

Yin, J.H., 2005. A consistent poleward shift of the storm tracks in simulations of 21st century climate. Geophysical Research Letters, 32(18).

DRAFT